Northern Hemisphere tropospheric ozone increases since the mid-1990s: evidence from IAGOS, remote surface sites and OMI/MLS (2004-2018)

Owen R. Cooper, Audrey Gaudel, Kai-Lan Chang
CIRES, University of Colorado/NOAA Earth System Research Laboratory, Boulder

Martin Schultz, Sabine Schröder
Jülich Supercomputing Centre (JSC), Forschungszentrum Jülich, Jülich, DE

Valerie Thouret, Philippe Nédélec
Laboratoire d'Aérologie, Université de Toulouse, CNRS, UPS, France

Jerry R. Ziemke,
NASA Goddard Space Flight Center, Greenbelt, Maryland, USA
Morgan State University, Baltimore, Maryland, USA

Sarah A. Strode
NASA Goddard Space Flight Center, Greenbelt, Maryland, USA
Universities Space Research Association, Columbia, Maryland, USA

The 2019 Aura Science Team Meeting
Hilton Pasadena, Pasadena, August 27-29, 2019

Four new papers on tropospheric ozone trends:

Tarasick, D., and I. E. Galbally et al. (2019), **Tropospheric Ozone Assessment Report: Tropospheric ozone from 1877 to 2016, observed levels, trends and uncertainties**, *Elementa: Science of the Anthropocene, in-press*

Cooper, O. R., M. G. Schultz, S. Schröder, K.-L. Chang, A. Gaudel, G. Carbajal Benítez, E. Cuevas, M. Fröhlich, I. E. Galbally, D. Kubistin, X. Lu, A. McClure-Begley, S. Molloy, P. Nédélec, J. O'Brien, S. J. Oltmans, I. Petropavlovskikh, L. Ries, I. Senik, K. Sjöberg, S. Solberg, T. G. Spain, W. Spangl, M. Steinbacher, D. Tarasick, V. Thouret, X. Xu (2019), **Multi-decadal surface ozone trends at globally distributed remote locations**, *in-review*

Gaudel, A., O. R. Cooper, K.-L. Chang, Ilann Bourgeois, Jerry R. Ziemke, Sarah A. Strode, Philippe Nedelec, Romain Blot, Valerie Thouret (2019), **Tropospheric ozone is still increasing across the Northern Hemisphere**, *in-review*

Ziemke, J. R., et al. (2019), **Trends in global tropospheric ozone inferred from a composite record of TOMS/OMI/MLS/OMPS satellite measurements and the MERRA-2 GMI simulation** , *Atmos. Chem. Phys., 19*, 3257-3269, https://doi.org/10.5194/acp-19-3257-2019, 2019.

The Tropospheric Ozone Assessment Report (TOAR)

TOAR-Observations [*Tarasick and Galbally et al.*, 2019] reviewed 60 historical surface ozone data sets, measured at rural locations world-wide, from 1896 to 1975.

These data were measured with methods developed before the advent of modern UV instruments (circa 1975), and therefore the values can be highly uncertain.

At northern mid- and high latitudes, ozone increased by 30-70% (with high uncertainty) from the mid-20th century to the present day (1990-2014).

We found no clear evidence for a doubling of ozone.

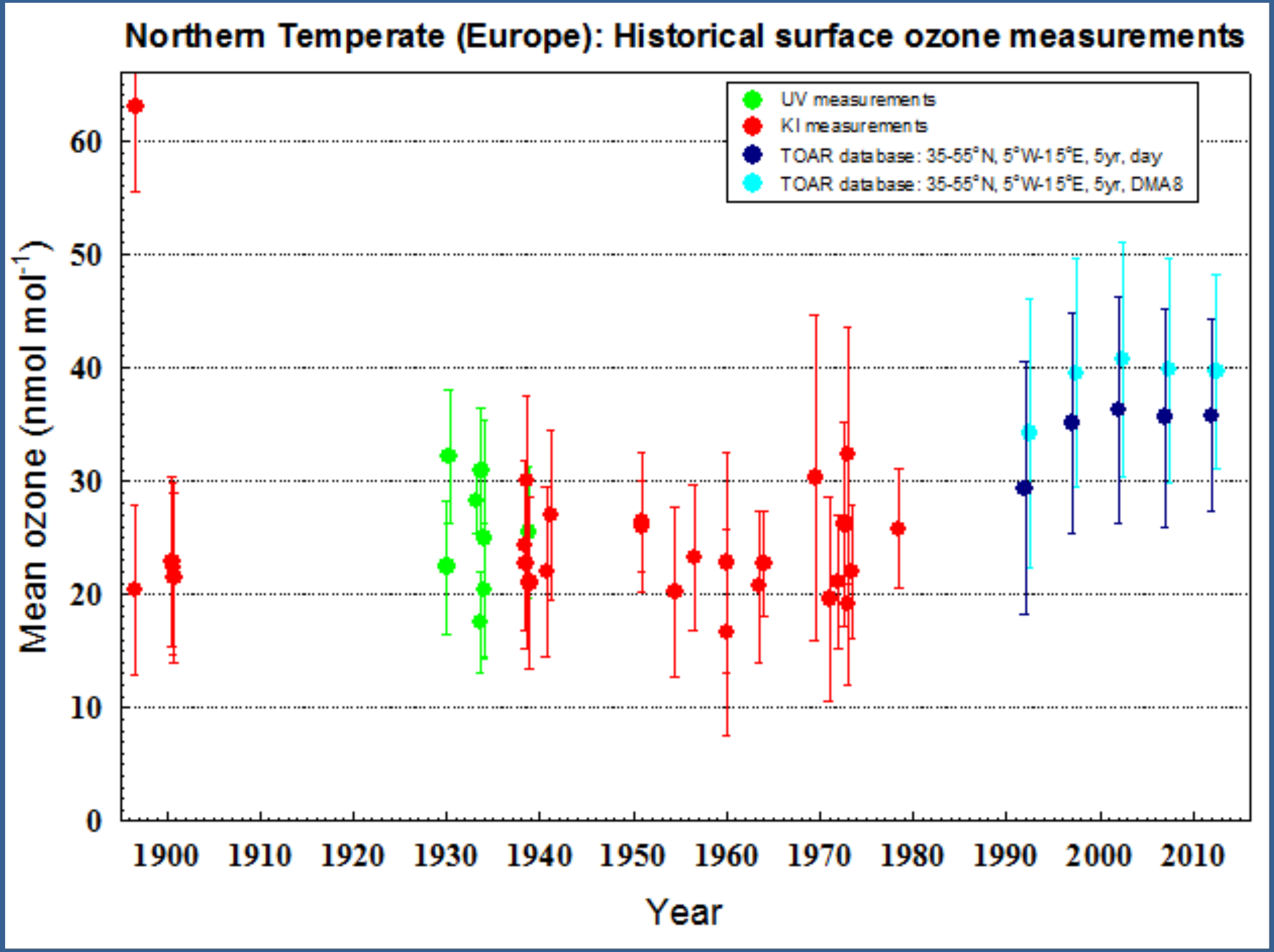

Cooper, O. R., et al. (2019), **Multi-decadal surface ozone trends at globally distributed remote locations**, *in-review*

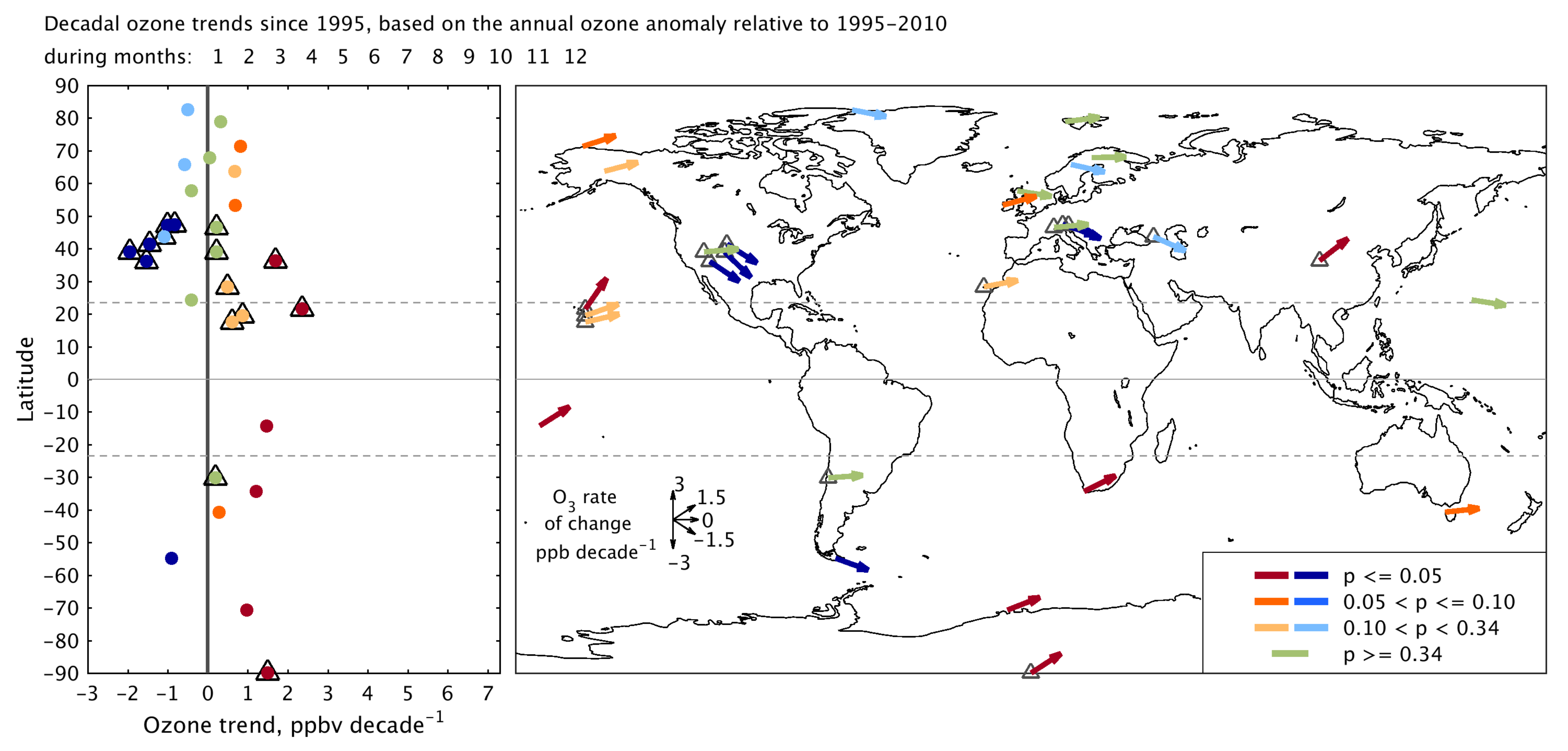

Severe surface ozone pollution in China: a global perspective

Xiao Lu, Jiayun Hong, Lin Zhang, Owen R. Cooper, Martin G. Schultz, Xiaobin Xu, Tao Wang, Meng Gao, Yuanhong Zhao, Yuanhang Zhang

Published in ES&T Letters, 2018

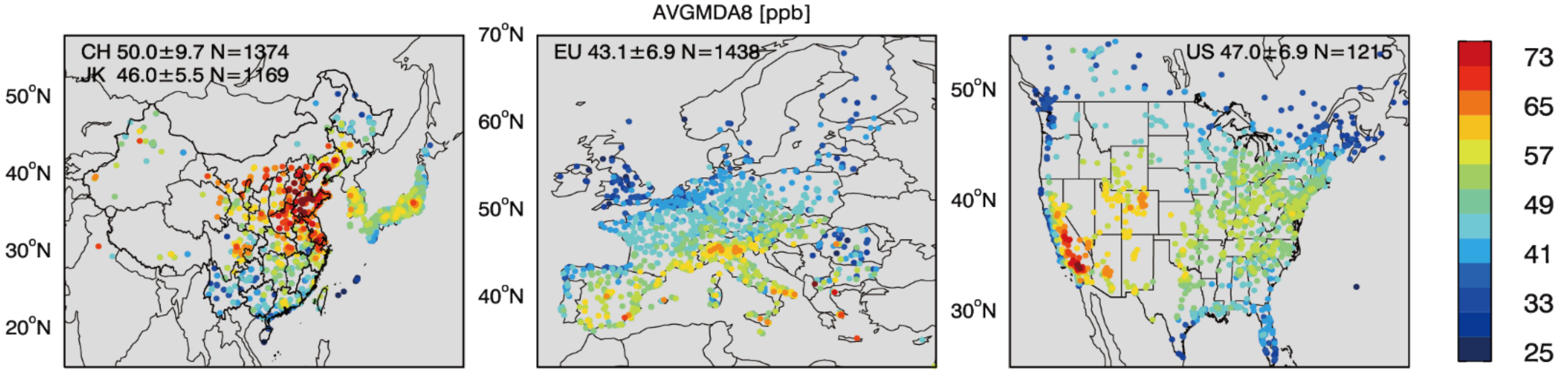

Summary of daytime average ozone values across China for the period 2013-2018.
Observations are averaged across 74 major Chinese cities during the months of April-September.

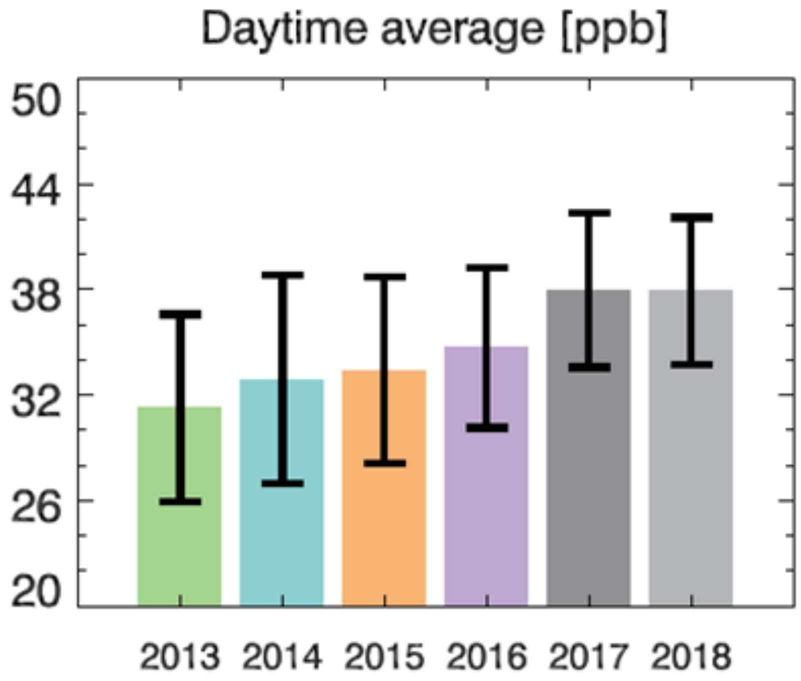

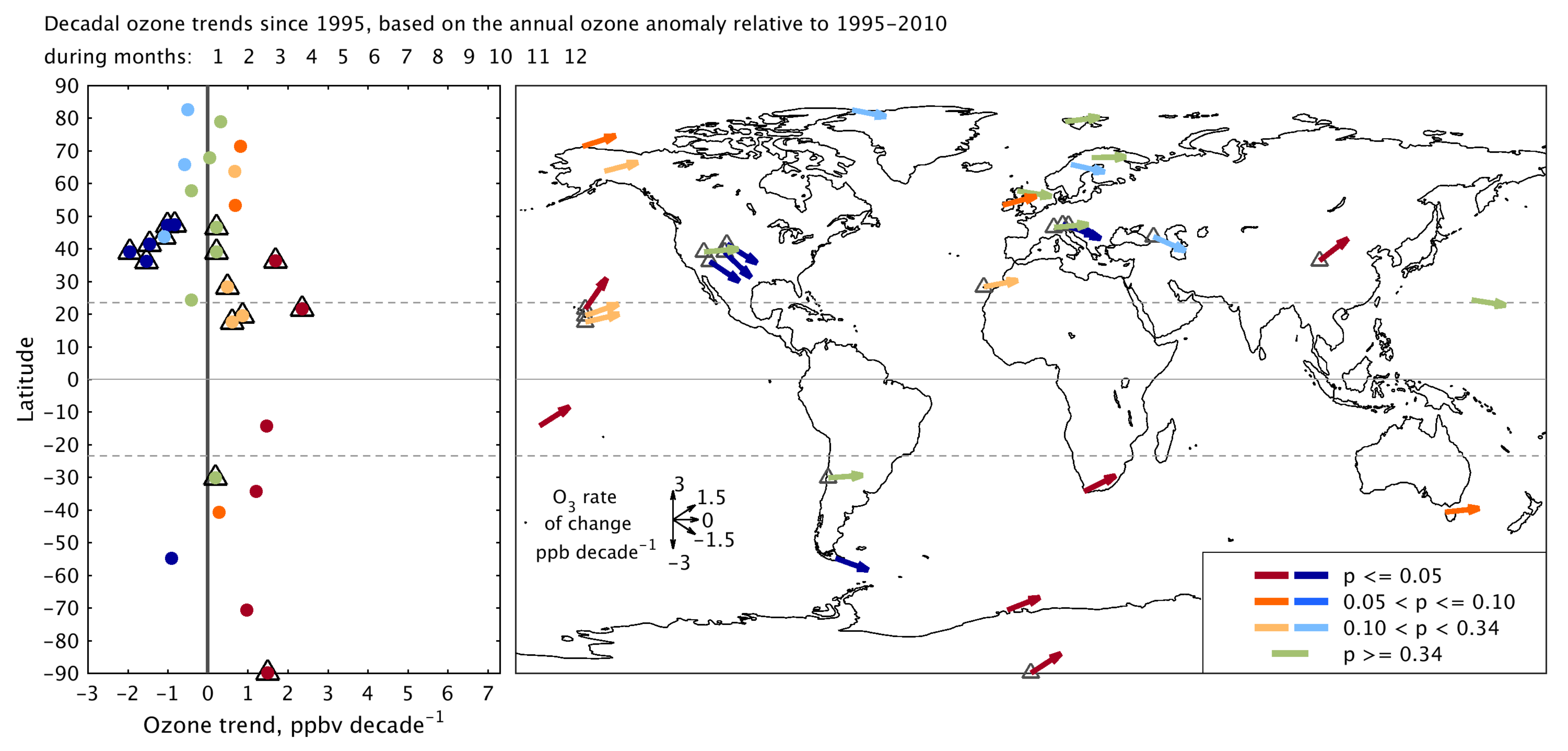

Decadal ozone trends since 1995, based on the annual ozone anomaly relative to 1995-2010
during months: 1 2 3 4 5 6 7 8 9 10 11 12
Latitude
Ozone trend, ppbv decade^{-1}
O_3 rate of change ppb decade^{-1}
3
1.5
0
−1.5
−3
p <= 0.05
0.05 < p <= 0.10
0.10 < p < 0.34
p >= 0.34

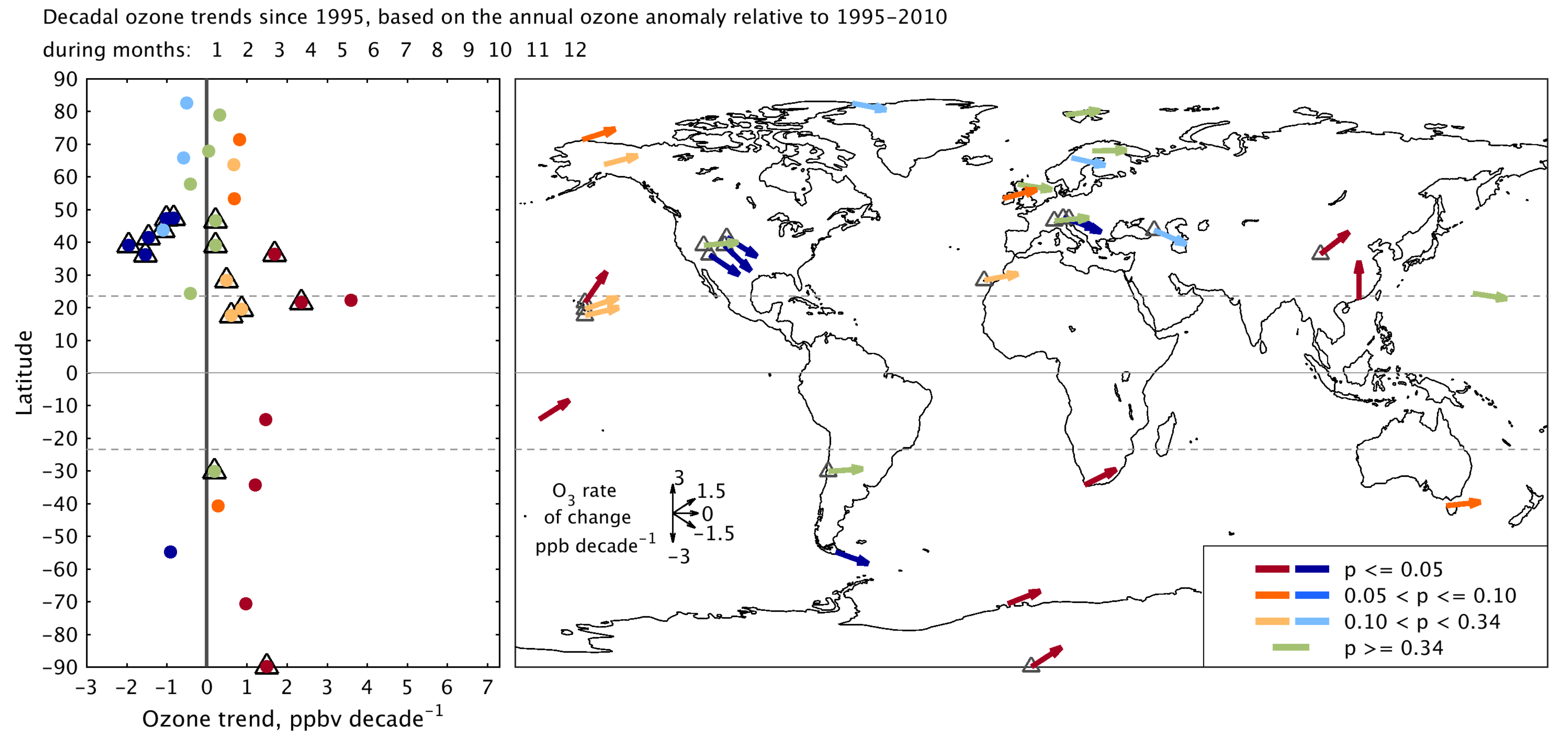

The baseline ozone trend at Hok Tsui near Hong Kong was provided by Prof. Tao Wang, Hong Kong Polytechnic

Gaudel, A., et al. (2019), **Tropospheric ozone is still increasing across the Northern Hemisphere**, *in-review*

Since 1994 IAGOS commercial aircraft have measured ozone worldwide with accurate UV instruments.

Eleven regions have sufficient data for trend analysis from 1994 to 2016.

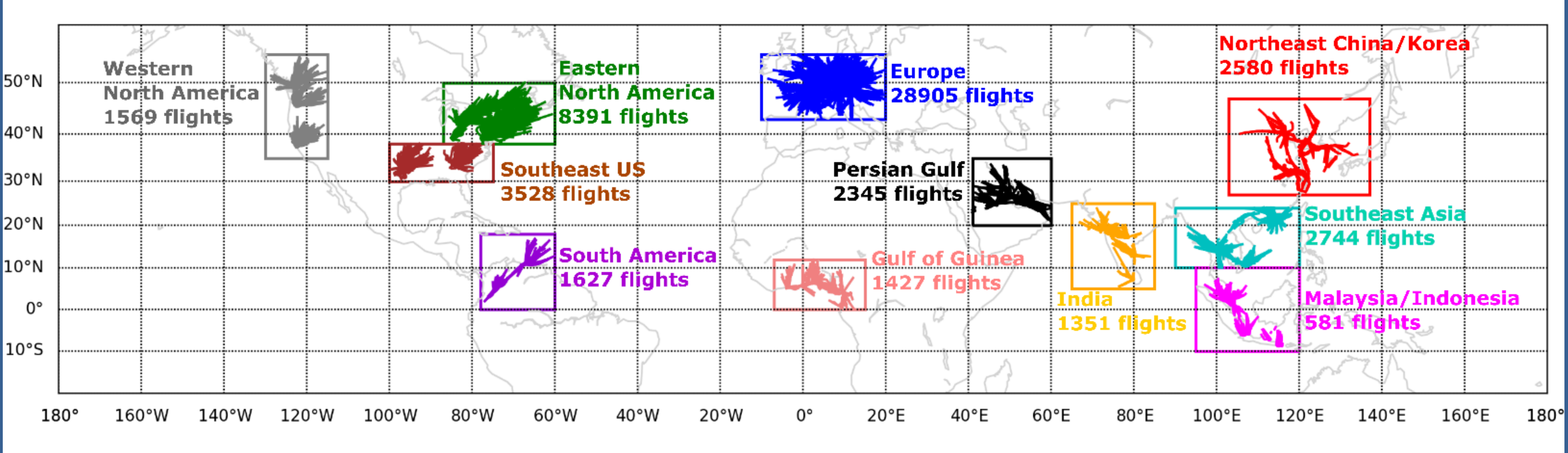

Free tropospheric ozone has increased above all eleven study regions.

Decreases in the boundary layer of North America have been offset by increases in the free troposphere.

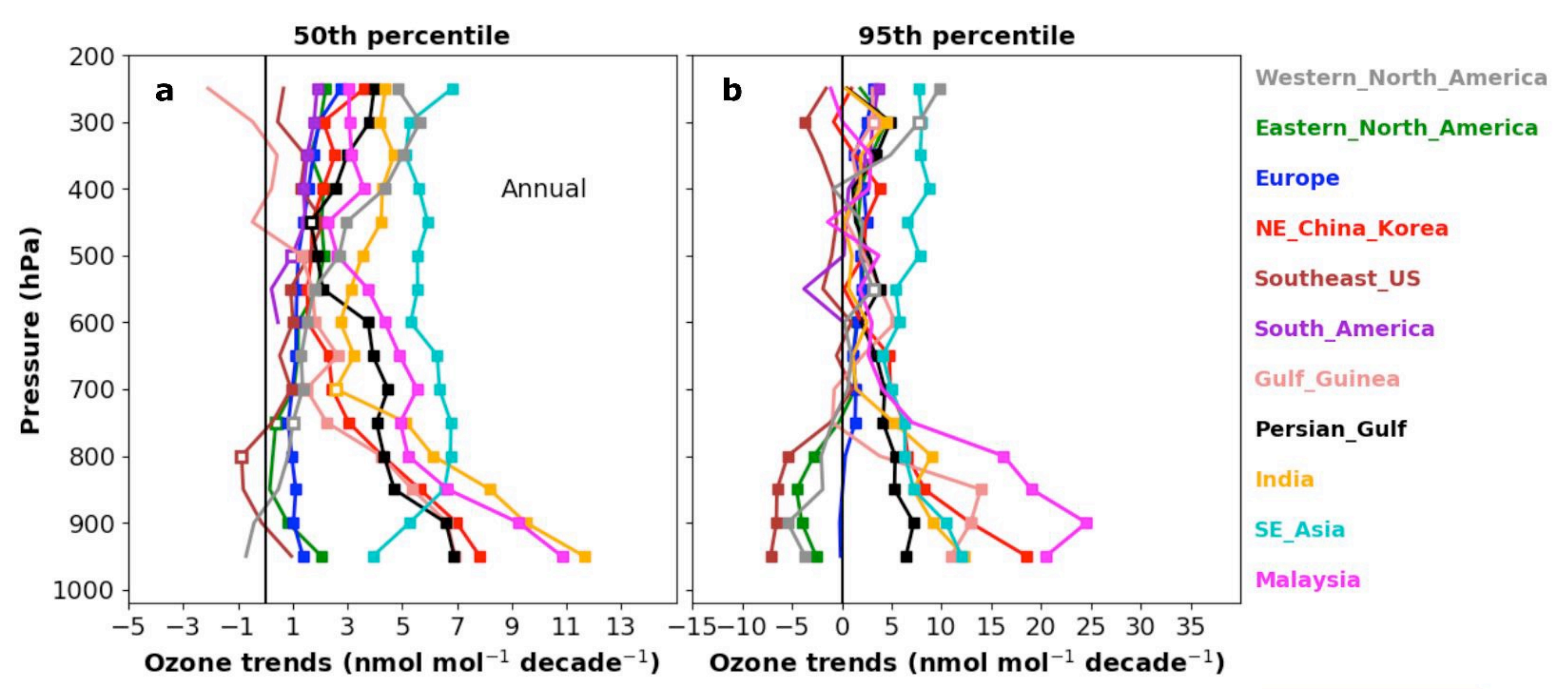

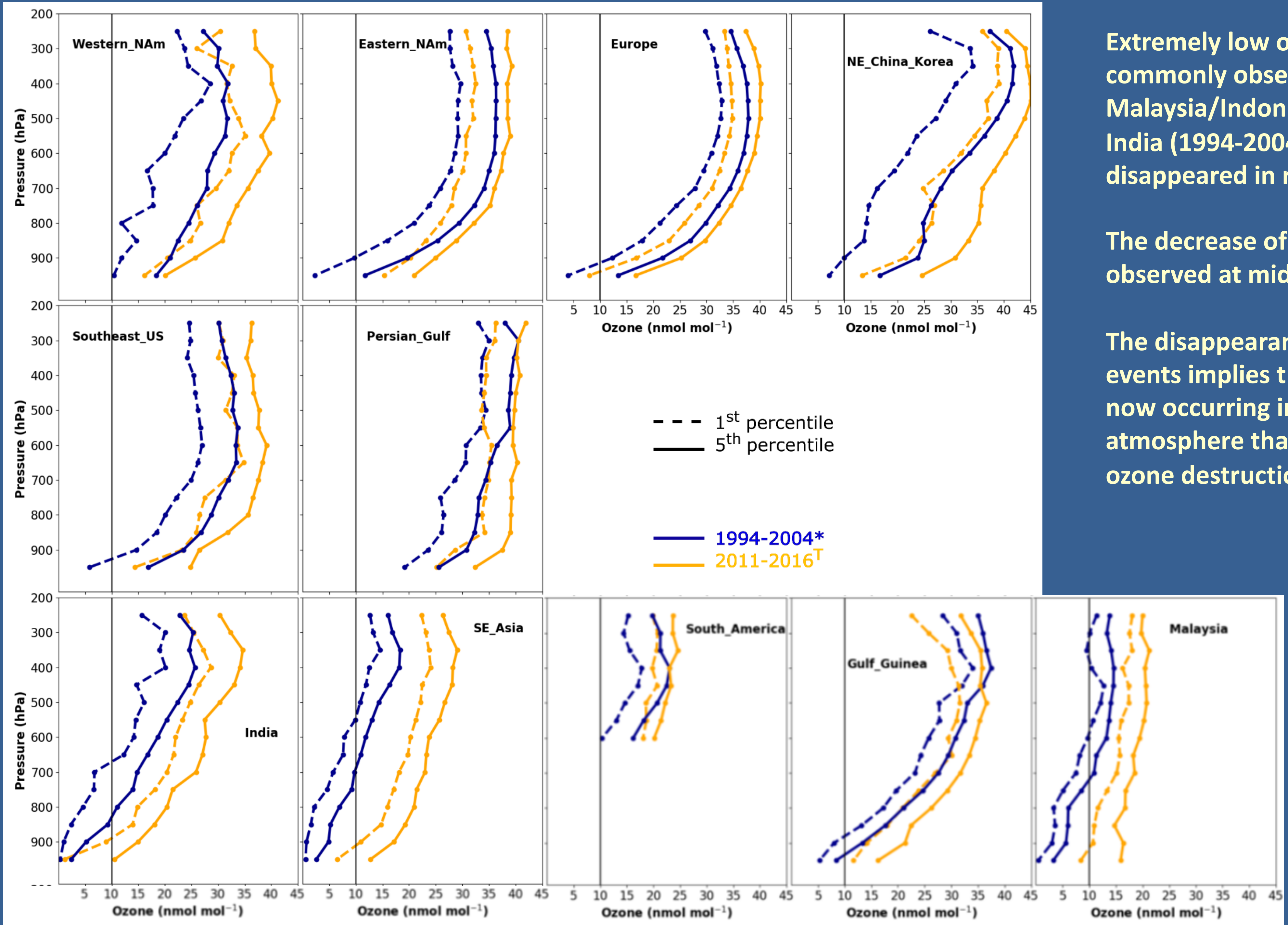

Extremely low ozone values once commonly observed above Malaysia/Indonesia, Southeast Asia and India (1994-2004) have almost completely disappeared in recent years (2011-2016).

The decrease of low ozone events is also observed at mid-latitudes.

The disappearance of the low ozone events implies that photochemistry is now occurring in remote regions of the atmosphere that were once dominated by ozone destruction.

Ozone trends at 27 rural surface sites, 1995-2018

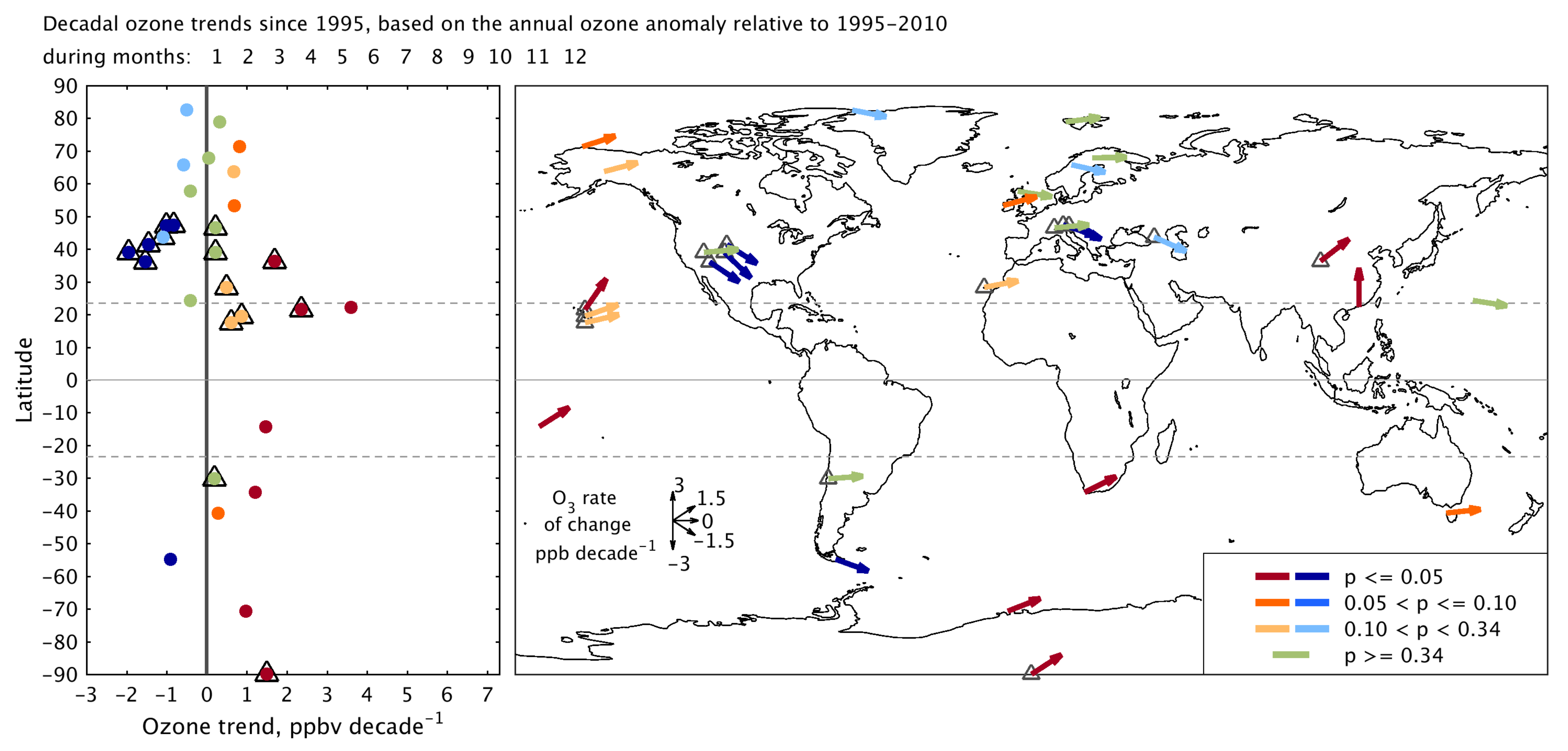

Ozone trends at 27 rural surface sites, 1995-2018,

plus IAGOS trends at 650 hPa, above 11 regions of the N. Hemisphere

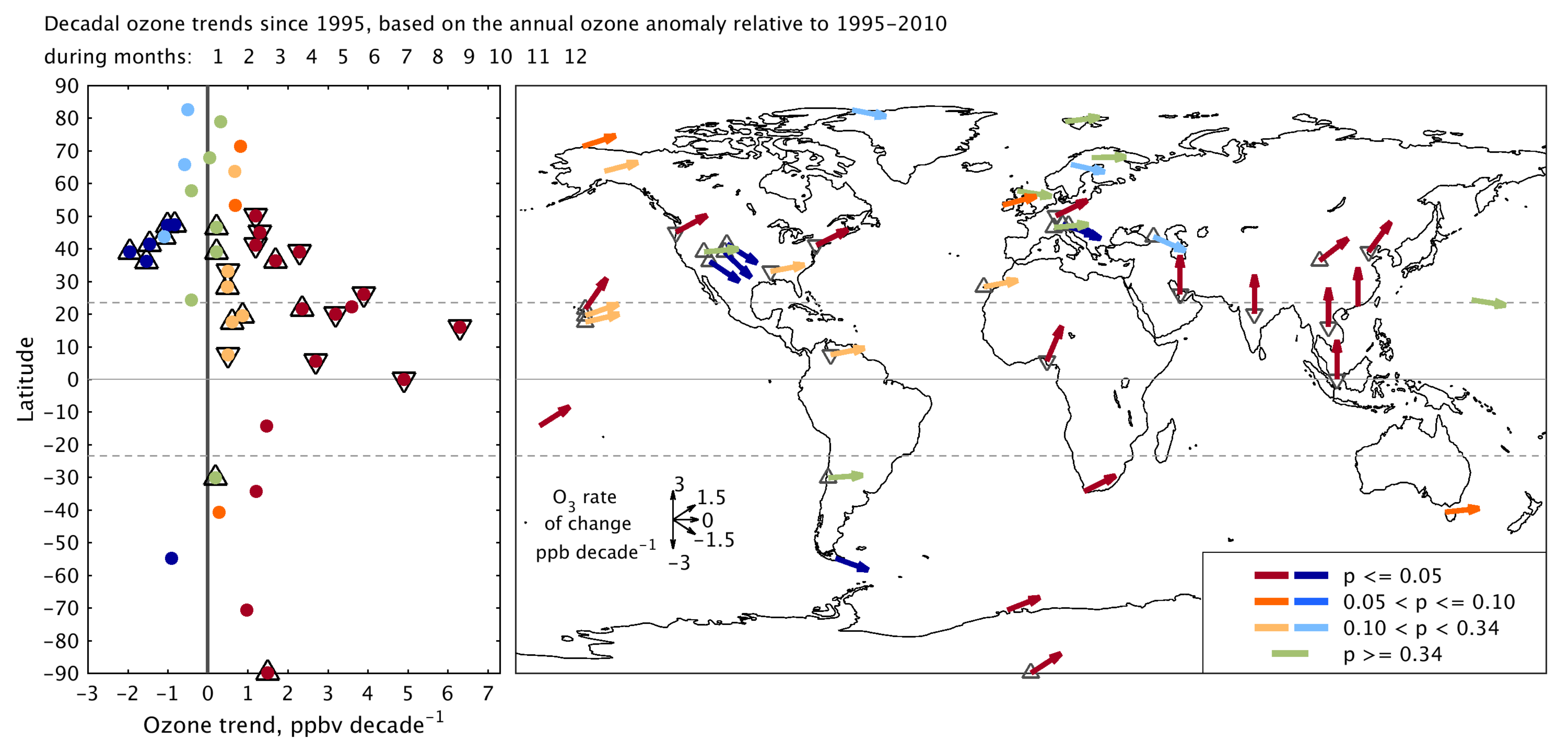

Ziemke, J. R., et al. (2019), **Trends in global tropospheric ozone inferred from a composite record of TOMS/OMI/MLS/OMPS satellite measurements and the MERRA-2 GMI simulation** , *Atmos. Chem. Phys., 19*, 3257-3269

The OMI/MLS product indicates a 9% increase in the tropospheric ozone burden from 2004 to 2018.

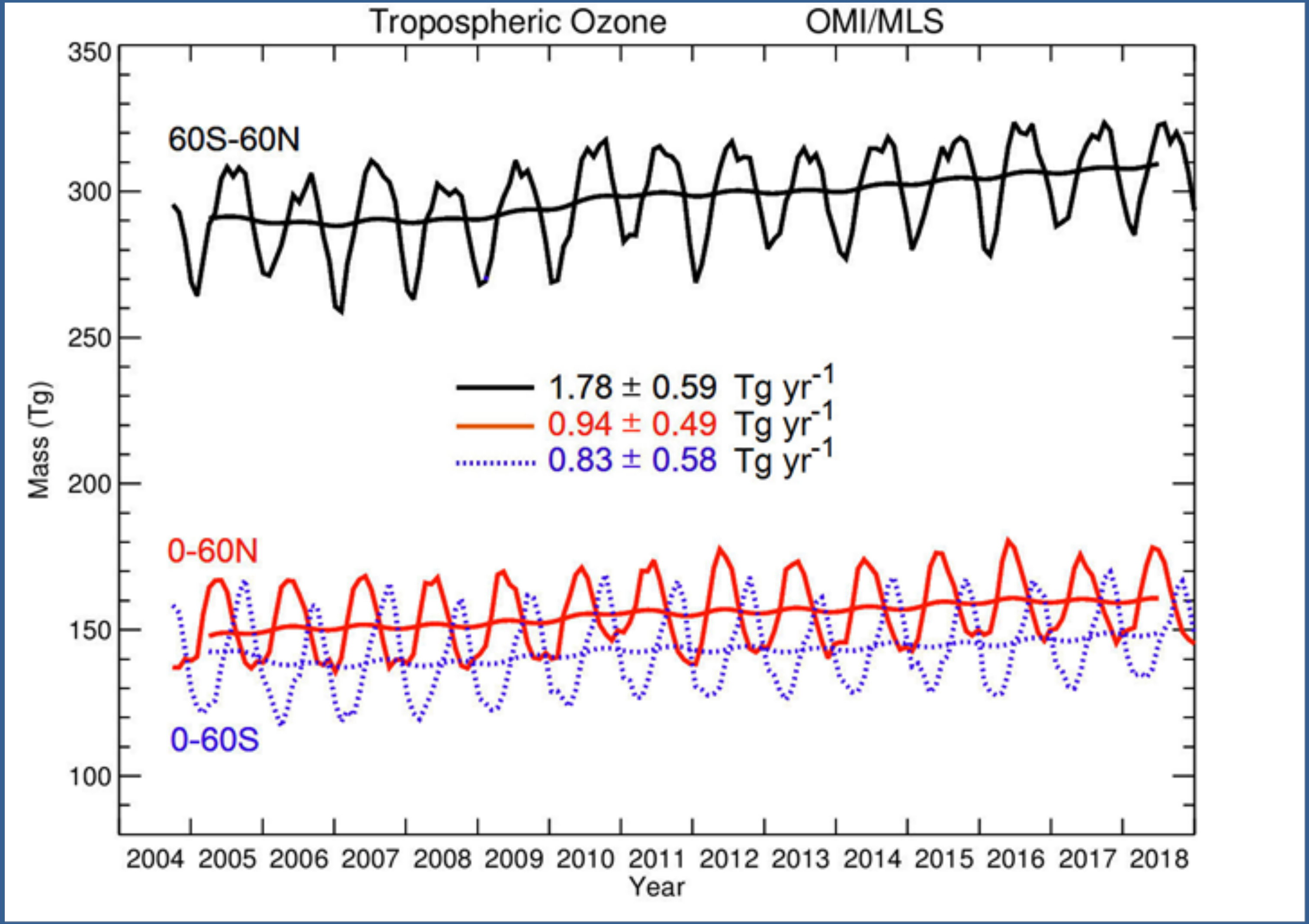

OMI/MLS trends for each 5x5 grid cell, 2004-2018.

Asterisks indicate trends with p-values < 0.05

IAGOS positive trends, 1994-2016

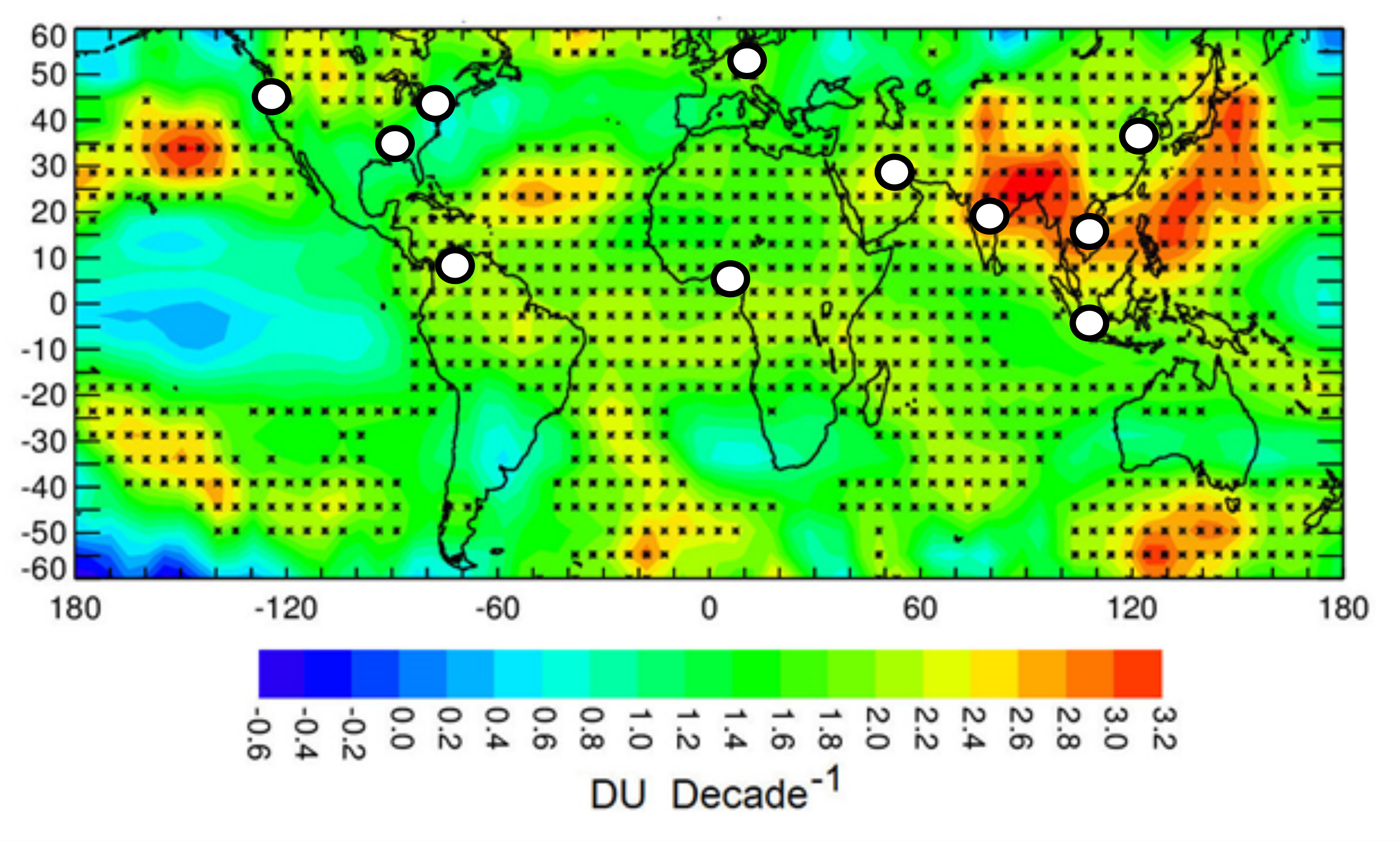

OMI/MLS trends compared to the NASA MERRA-GMI model, 2005-2016.

Asterisks indicate trends with p-values < 0.05

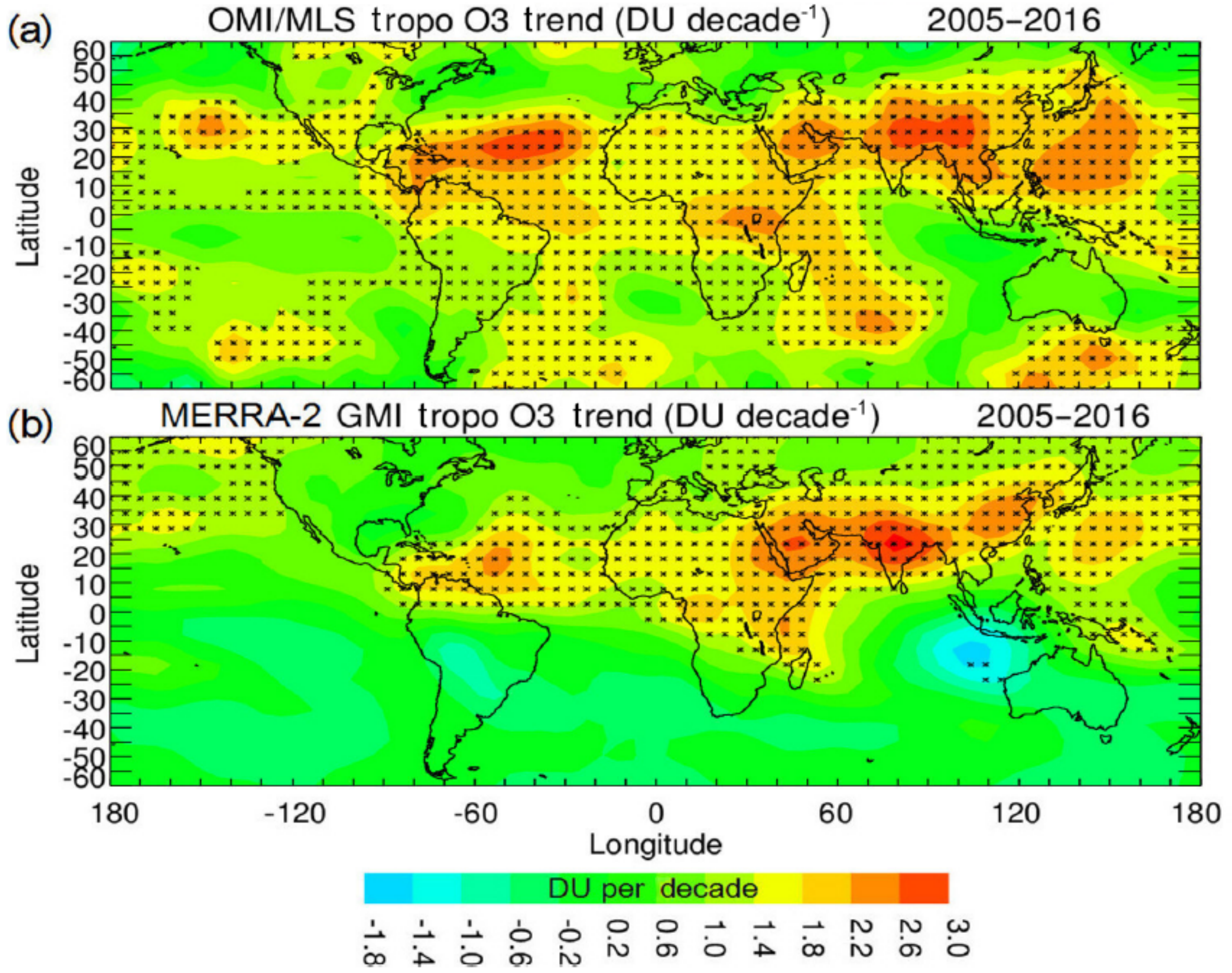

Figure 1. **(a)** Trends in OMI/MLS TCO (in DU decade^{-1}) for 2005–2016. Asterisks denote grid points where trends are statistically significant at the 2σ level. **(b)** Same as **(a)** except for MERRA-2 GMI TCO.

Additional slides for discussion

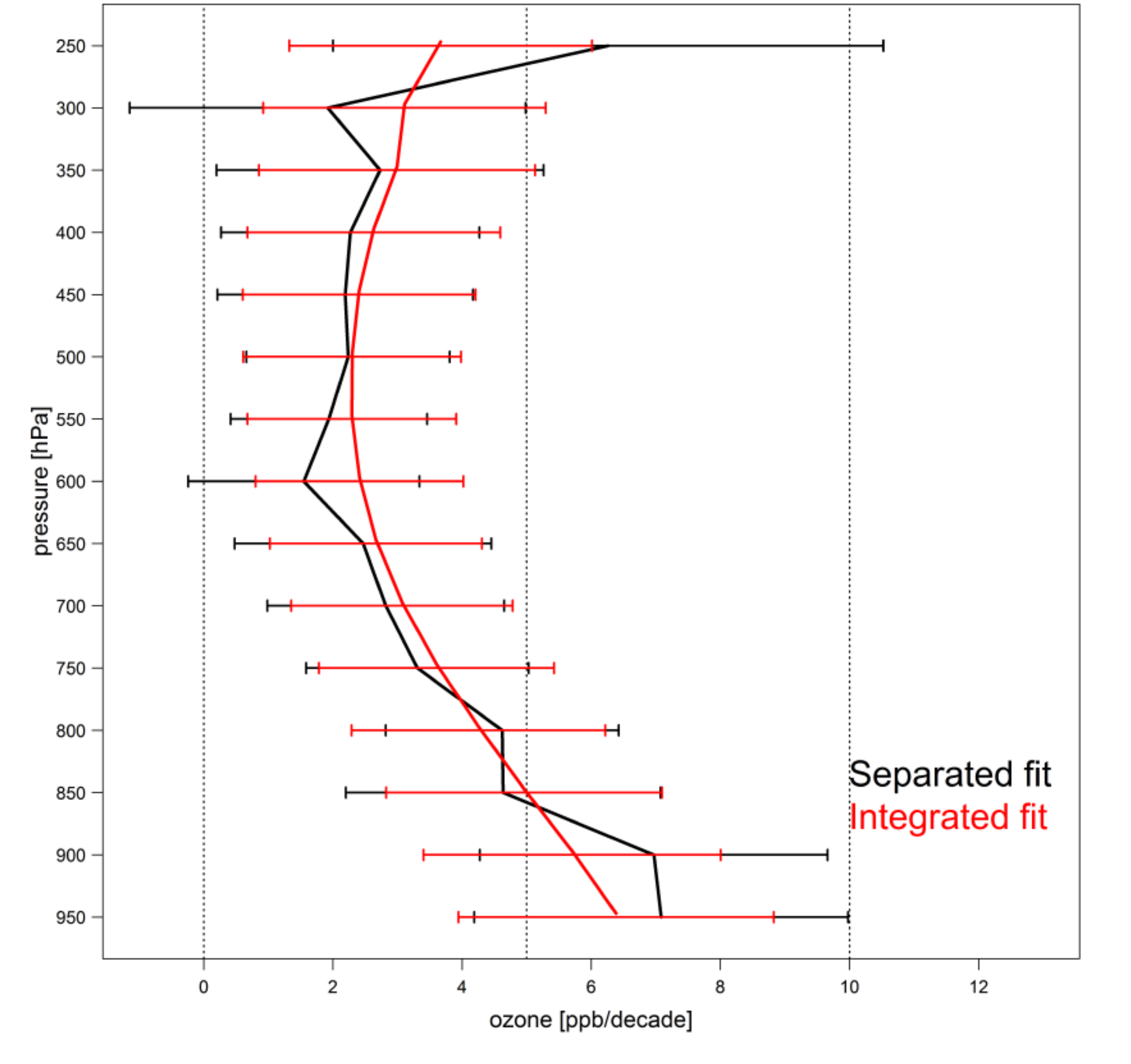

Figure 9. Tropospheric ozone trend estimates and associated 2-sigma variabilities at 50hPa vertical resolution from individual linear regression in Eq (1) and smoothing spline decomposition in Eq (2) in China.

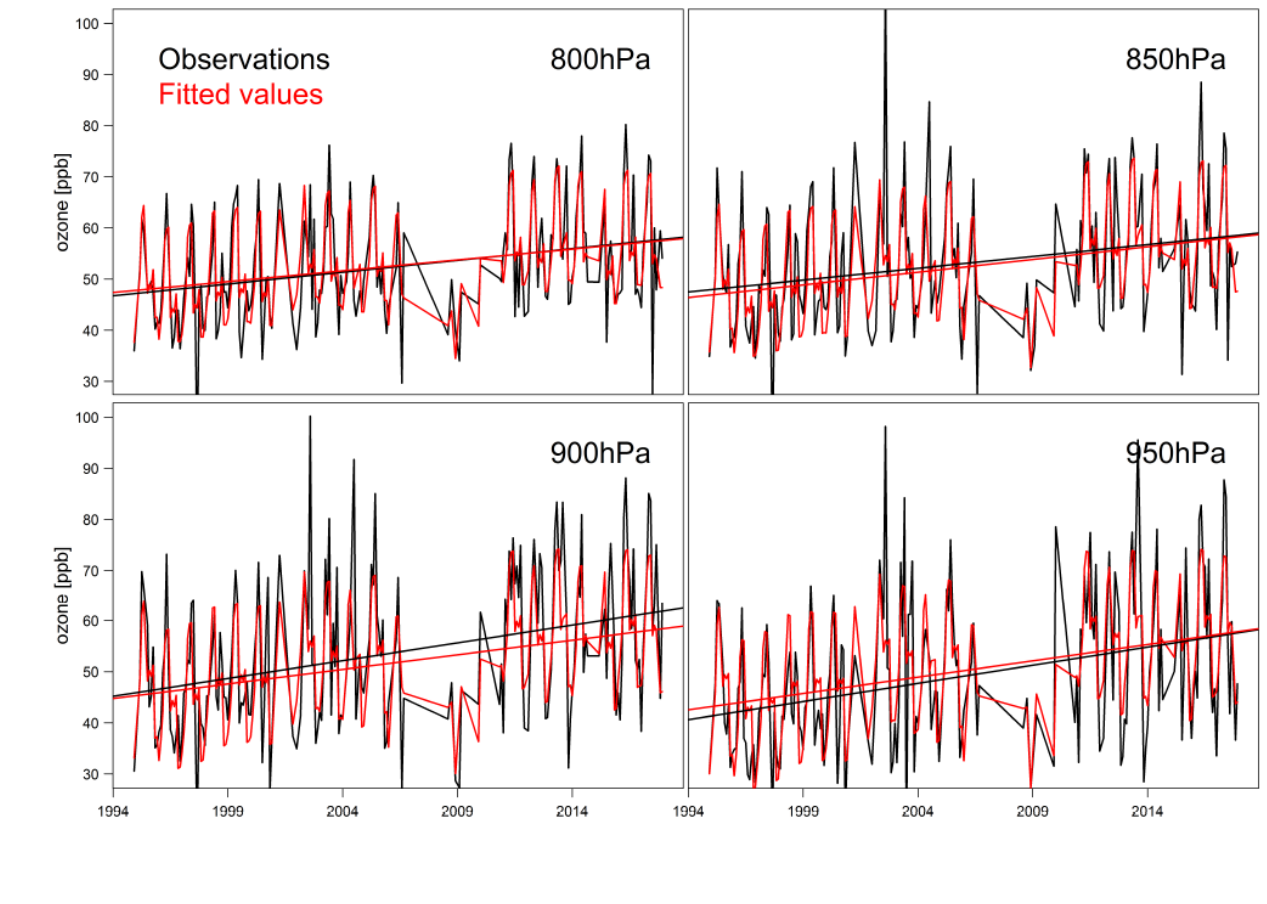

Figure A6. Tropospheric ozone time series and model fitted values at 4 lower layers in China.

IAGOS ozone trends above northeastern China, 1994-2016.

Chang, K.-L., et al. (2019), Statistical regularization for trend detection: An integrated approach for detecting long-term trends from sparse tropospheric ozone profiles, *in preparation.*

IAGOS ozone trends above Hilo, Hawaii China, 1982-2018.

Chang, K.-L., et al. (2019), Statistical regularization for trend detection: An integrated approach for detecting long-term trends from sparse tropospheric ozone profiles, *in preparation.*

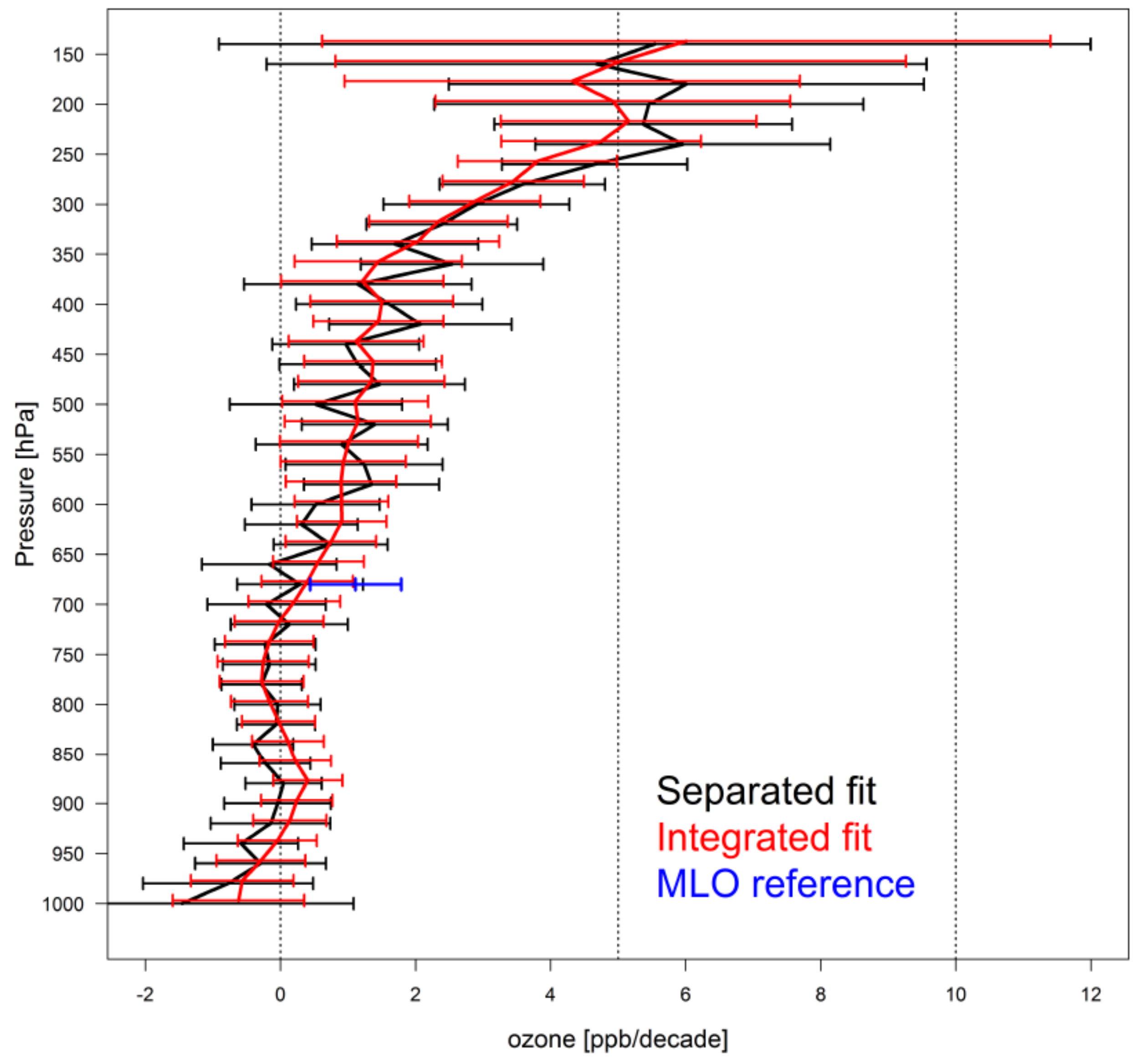

(a) Hilo, Hawaii (1982-2018)

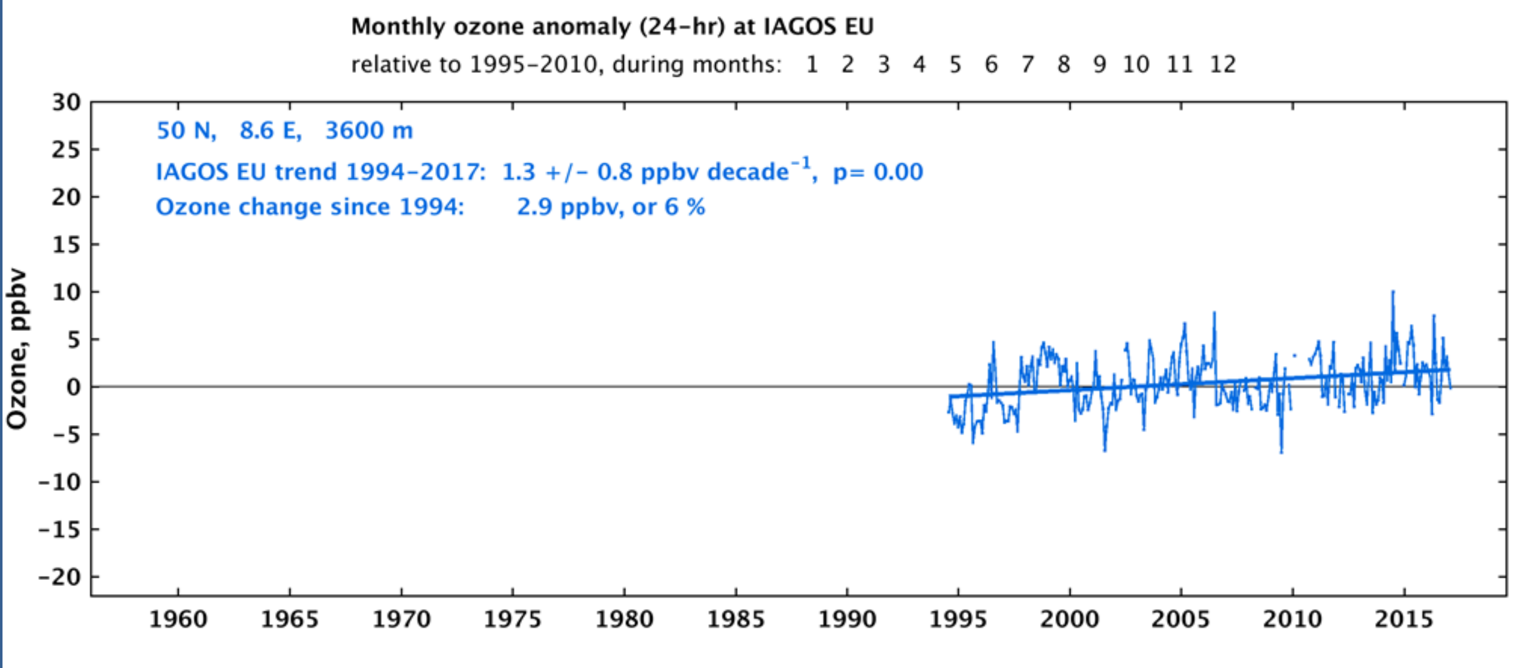

Monthly ozone anomaly (24-hr) at IAGOS EU
relative to 1995-2010, during months: 1 2 3 4 5 6 7 8 9 10 11 12
50 N, 8.6 E, 3600 m
IAGOS EU trend 1994-2017: 1.3 +/- 0.8 ppbv decade^{-1}, p= 0.00
Ozone change since 1994: 2.9 ppbv, or 6 %
Ozone, ppbv
30
25
20
15
10
5
0
-5
-10
-15
-20
1960
1965
1970
1975
1980
1985
1990
1995
2000
2005
2010
2015

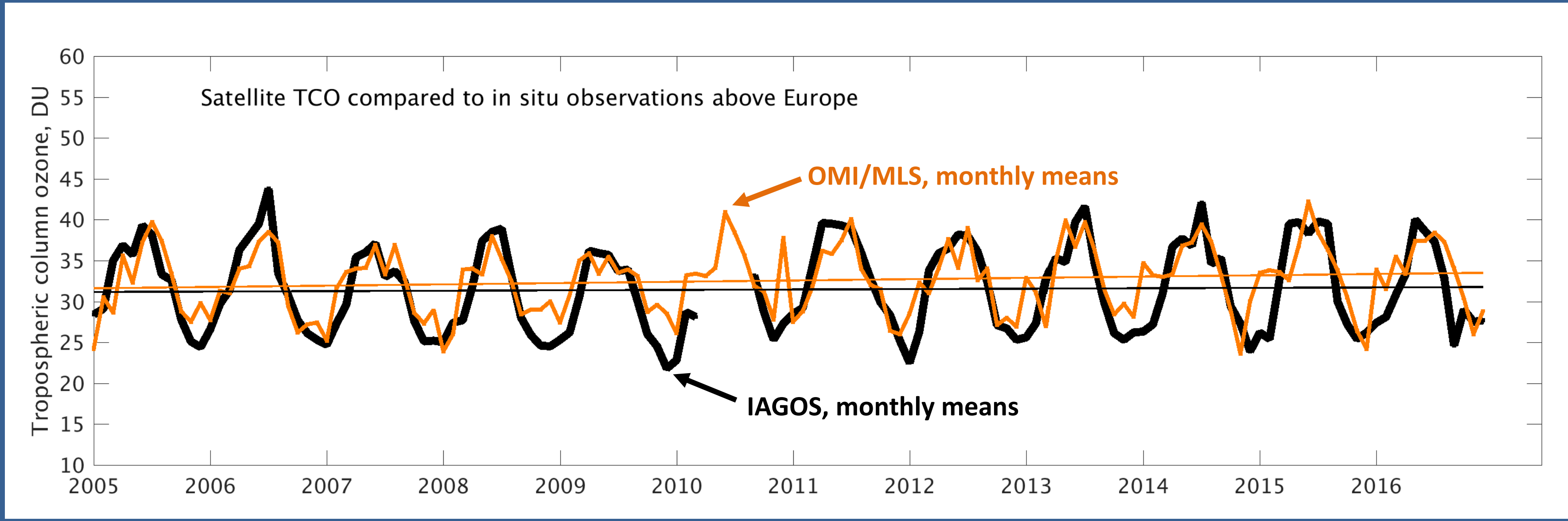

Satellite TCO compared to in situ observations above Europe
OMI/MLS, monthly means
IAGOS, monthly means
Tropospheric column ozone, DU
60
55
50
45
40
35
30
25
20
15
10
2005
2006
2007
2008
2009
2010
2011
2012
2013
2014
2015
2016

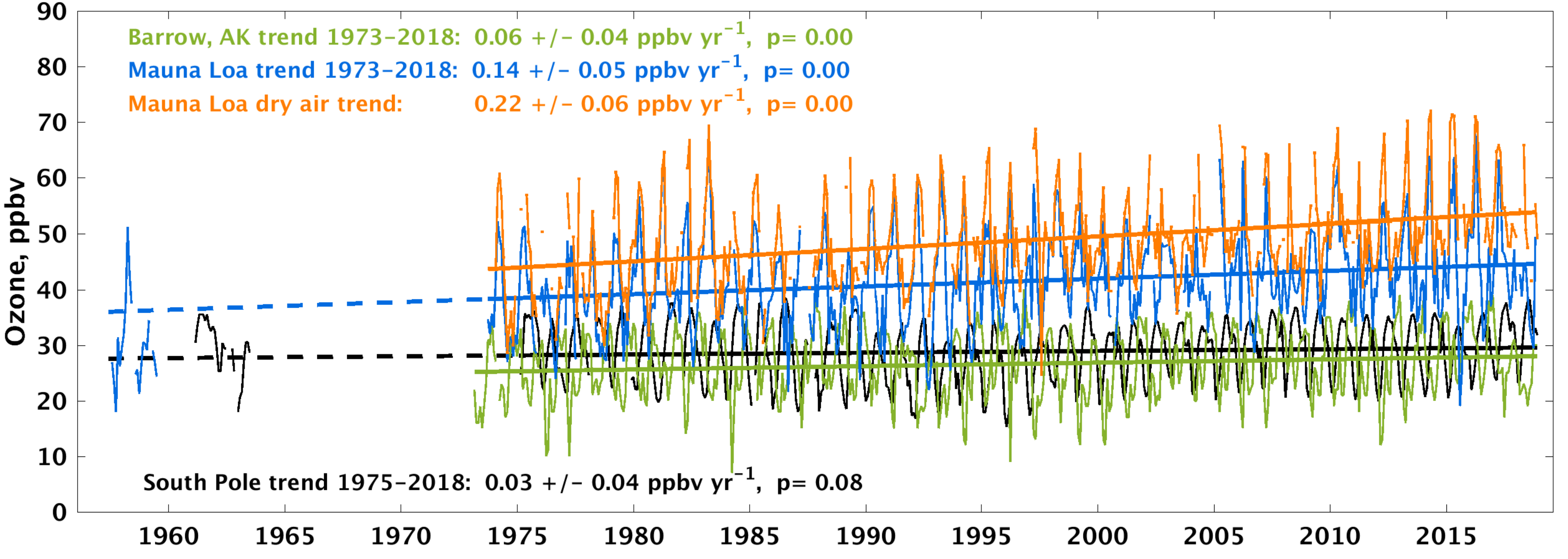

Barrow, AK trend 1973-2018: 0.06 +/- 0.04 ppbv yr^{-1}, p= 0.00
Mauna Loa trend 1973-2018: 0.14 +/- 0.05 ppbv yr^{-1}, p= 0.00
Mauna Loa dry air trend: 0.22 +/- 0.06 ppbv yr^{-1}, p= 0.00
South Pole trend 1975-2018: 0.03 +/- 0.04 ppbv yr^{-1}, p= 0.08
Ozone, ppbv
0
10
20
30
40
50
60
70
80
90
1960
1965
1970
1975
1980
1985
1990
1995
2000
2005
2010
2015

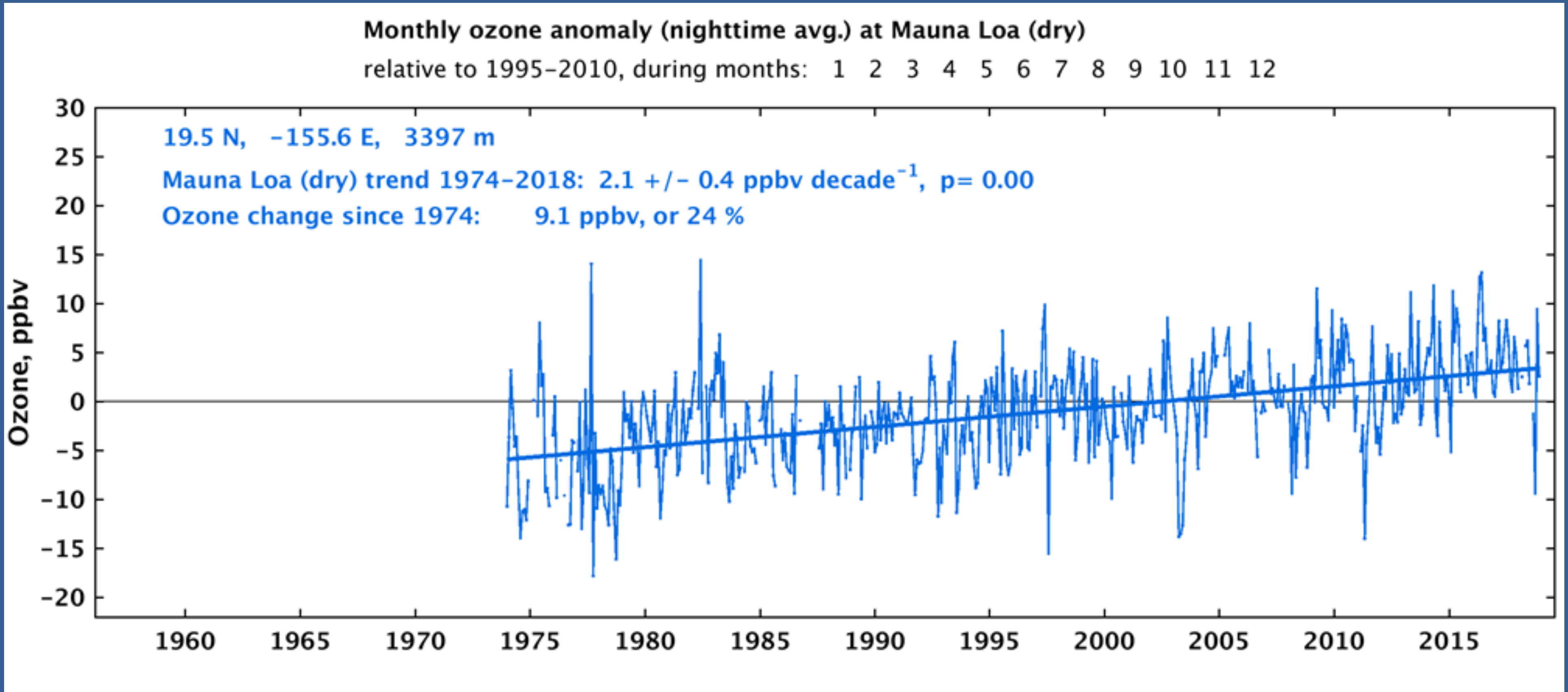

Monthly ozone anomaly (nighttime avg.) at Mauna Loa (dry)
relative to 1995-2010, during months: 1 2 3 4 5 6 7 8 9 10 11 12
19.5 N, -155.6 E, 3397 m
Mauna Loa (dry) trend 1974-2018: 2.1 +/- 0.4 ppbv decade^{-1}, p= 0.00
Ozone change since 1974: 9.1 ppbv, or 24 %
Ozone, ppbv
30
25
20
15
10
5
0
-5
-10
-15
-20
1960
1965
1970
1975
1980
1985
1990
1995
2000
2005
2010
2015

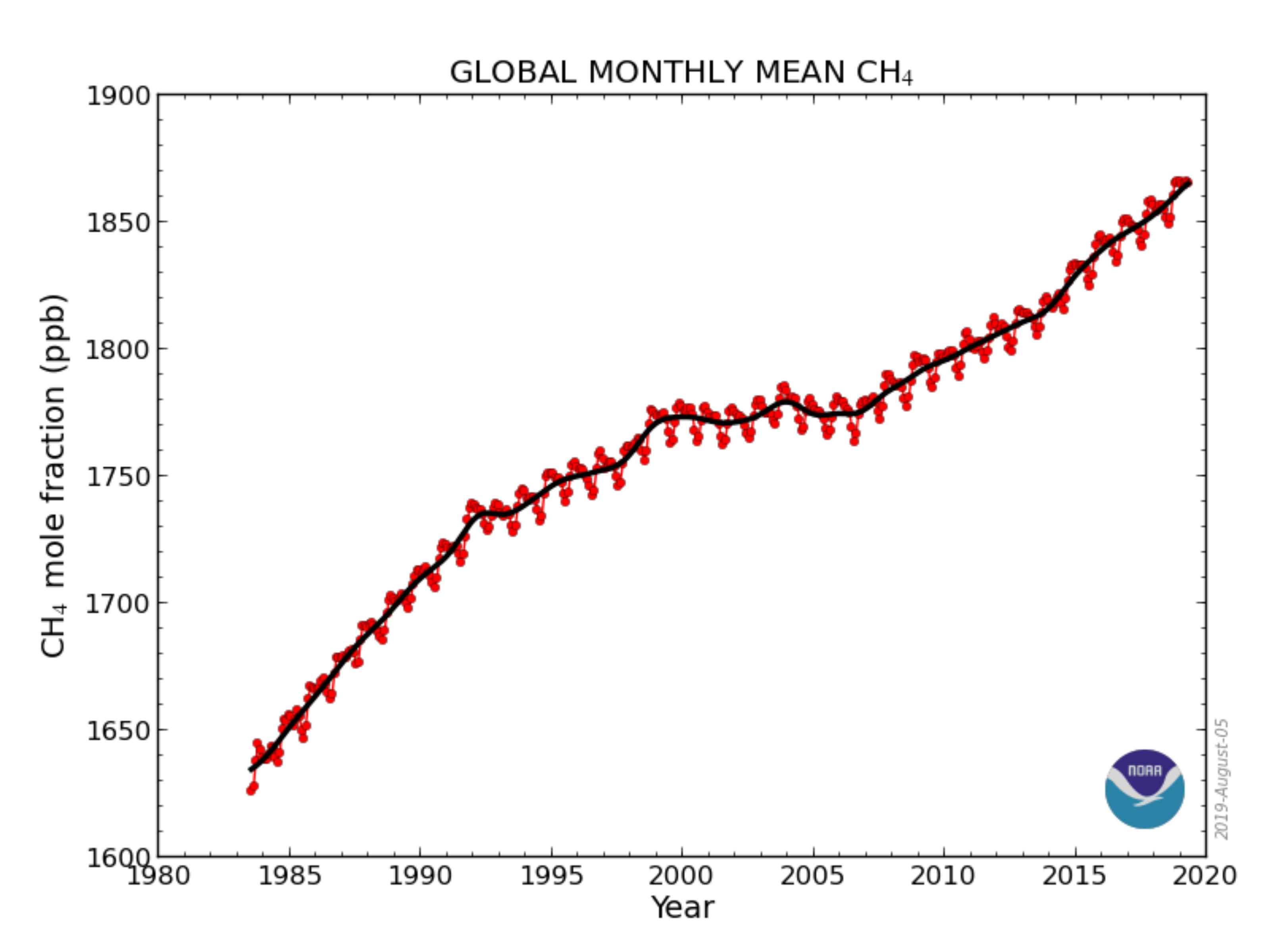

Methane has increased by 5% since Aura was launched in 2004

Tropospheric column ozone trends:

ozonesondes (TOST)
OMI/MLS
OMI (HSCfA)
OMI (RAL)
IASI (FORLI)
IASI (SOFRID)

Grid cells with white dots have statistically significant trends

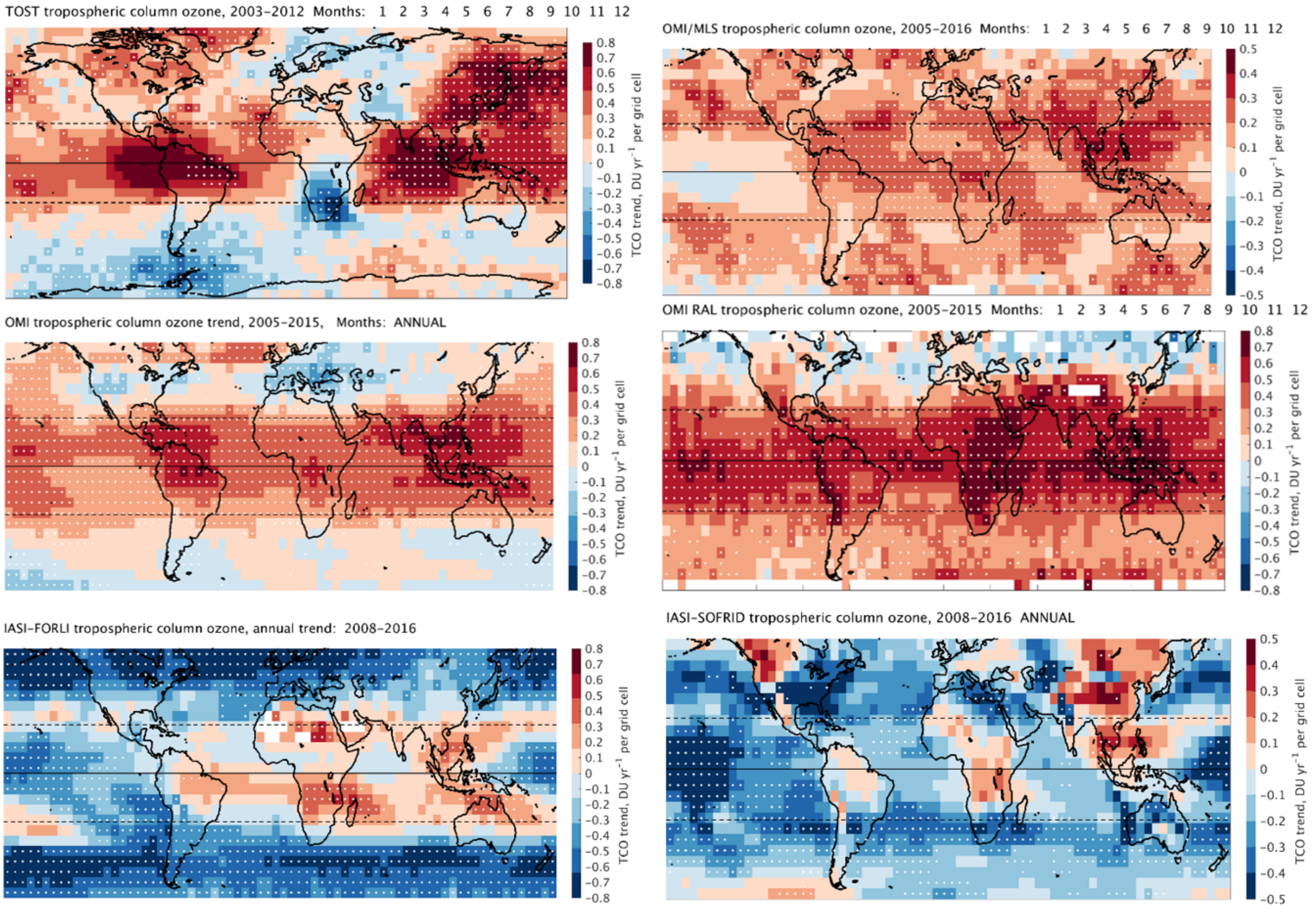

+ 5%

+ 5%

- 11%

- 17%

Satellite products disagree on the trend of the global tropospheric ozone burden.

In recent years the estimates have converged within ± 4%.

Satellite estimated ozone burden, 60° S – 60° N:

300 ± 12 Tg

ACCMIP model ensemble estimate:

299 ± 21 Tg

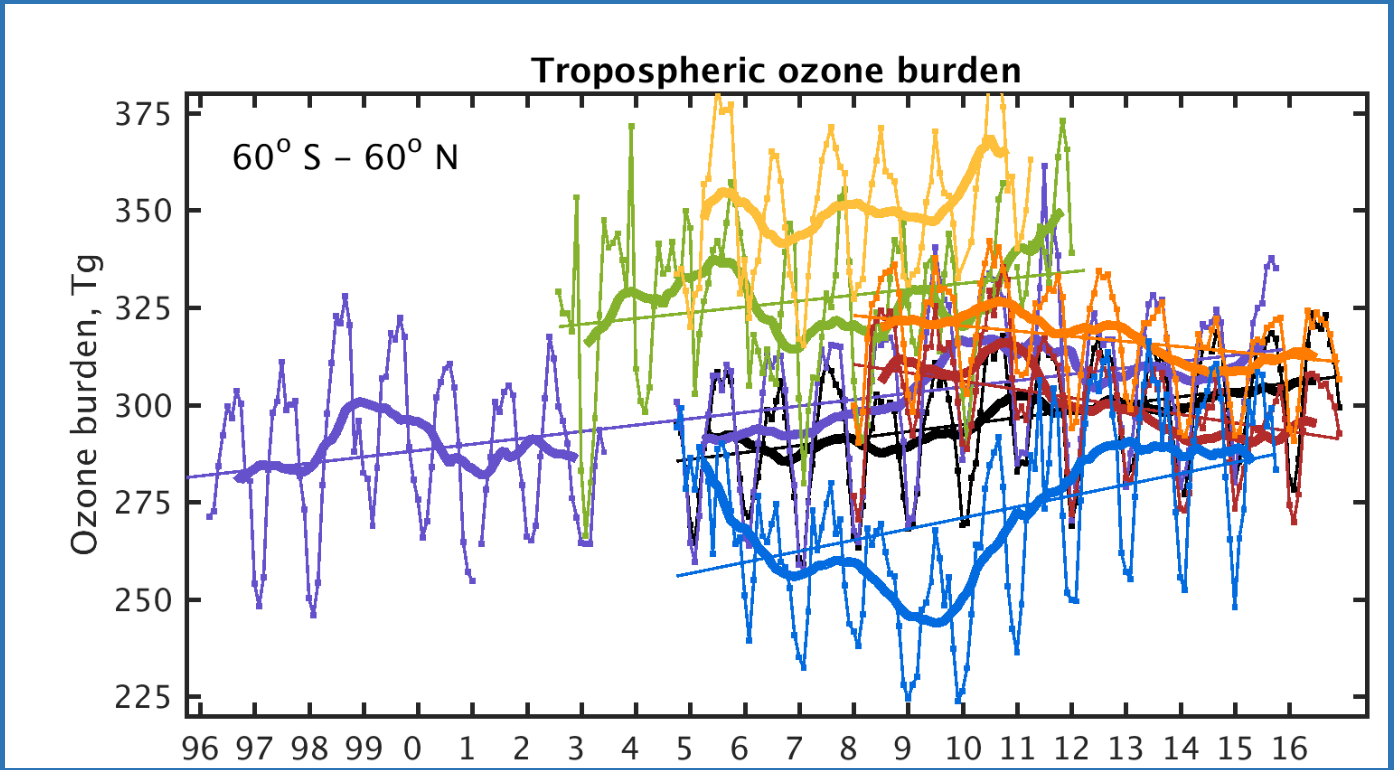

	change, Tg yr^{-1}	p-value
Black: OMI/MLS	1.79 +/- 0.66	0.00
Brown: IASI-FORLI	-2.15 +/- 1.03	0.00
Orange: IASI-SOFRID	-1.34 +/- 0.92	0.00
Purple: GOME/OMI	1.63 +/- 0.45	0.00
Blue: OMI-RAL	2.85 +/- 1.16	0.00
Green: SCIAMACHY	1.50 +/- 1.39	0.03
Yellow: TES		

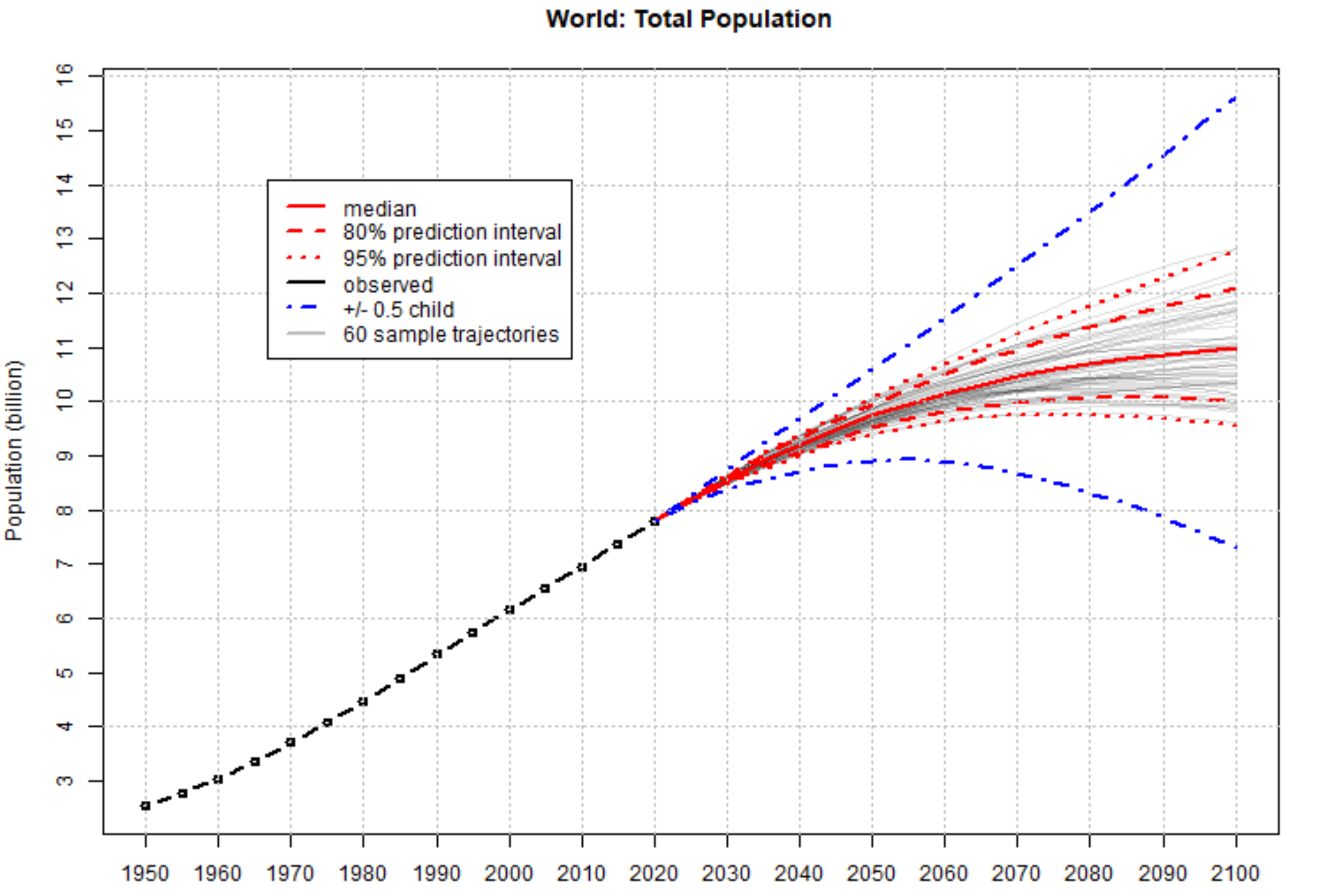

United Nations, DESA, Population Division. *World Population Prospects 2019*. http://population.un.org/wpp/

Global CO_2 emissions through 2018

Le Quéré et al., Global Carbon Budget 2018, Earth Syst. Sci. Data, 10, 2141-2194, 2018.

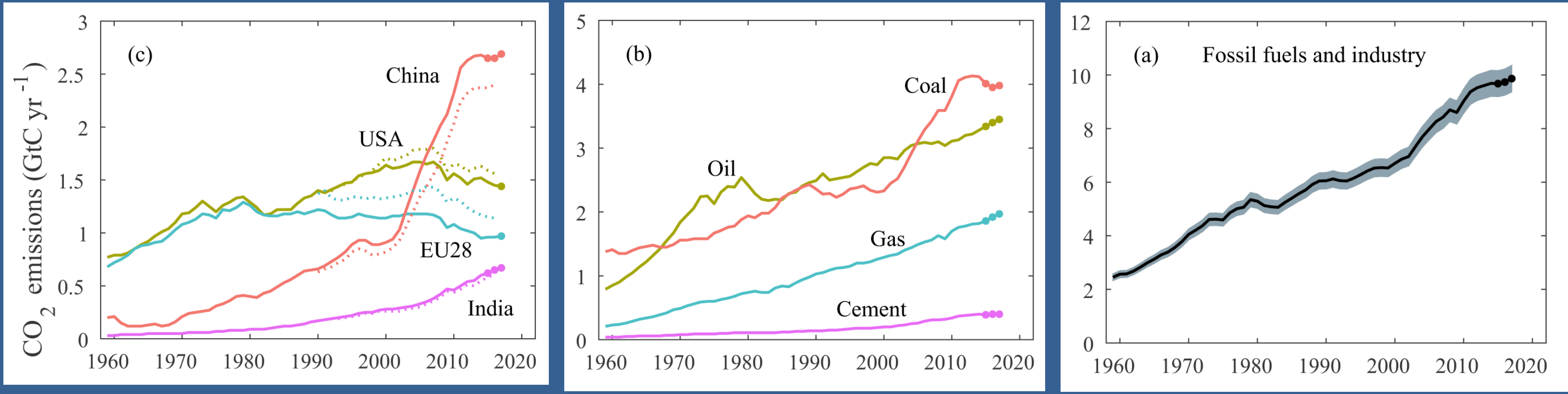

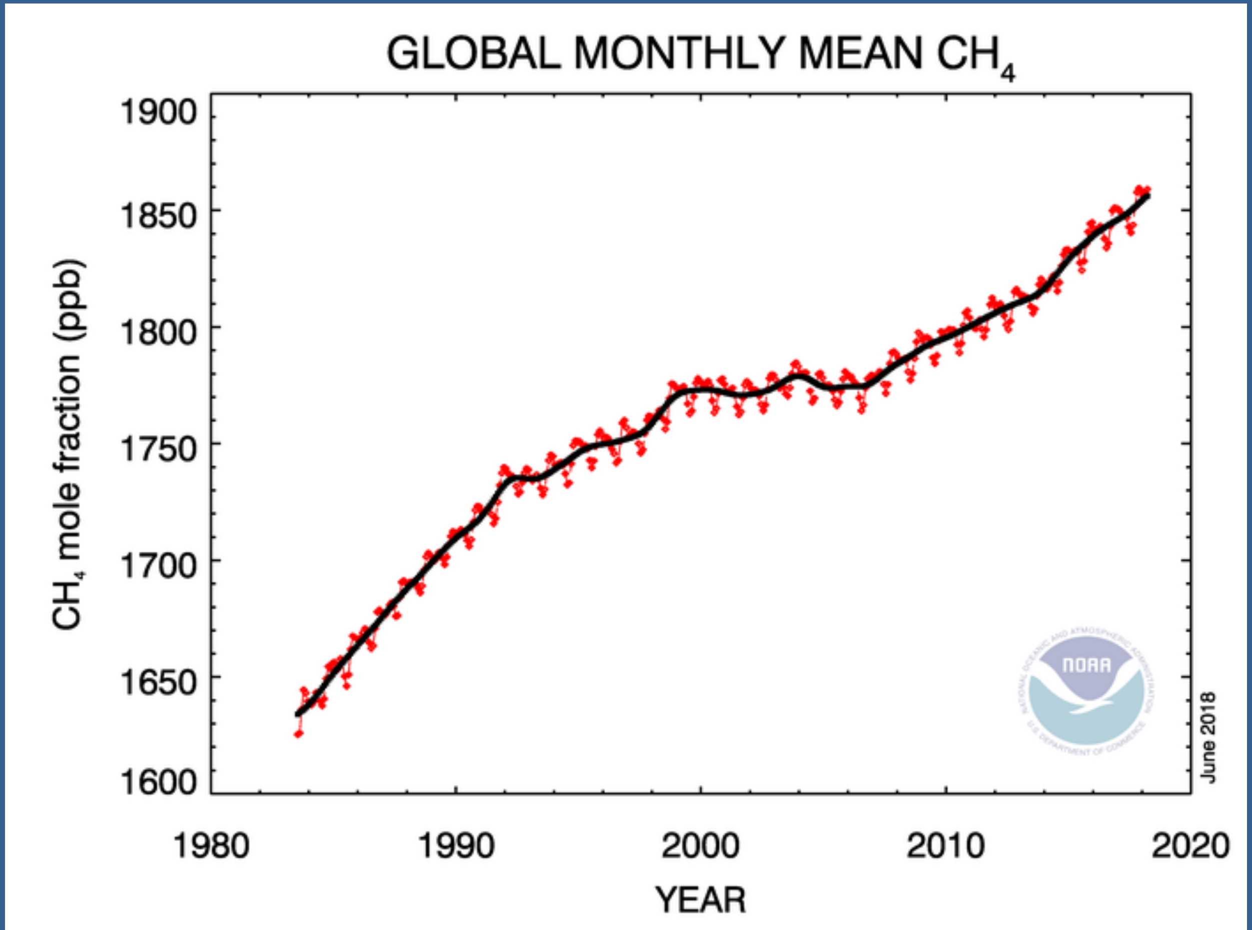

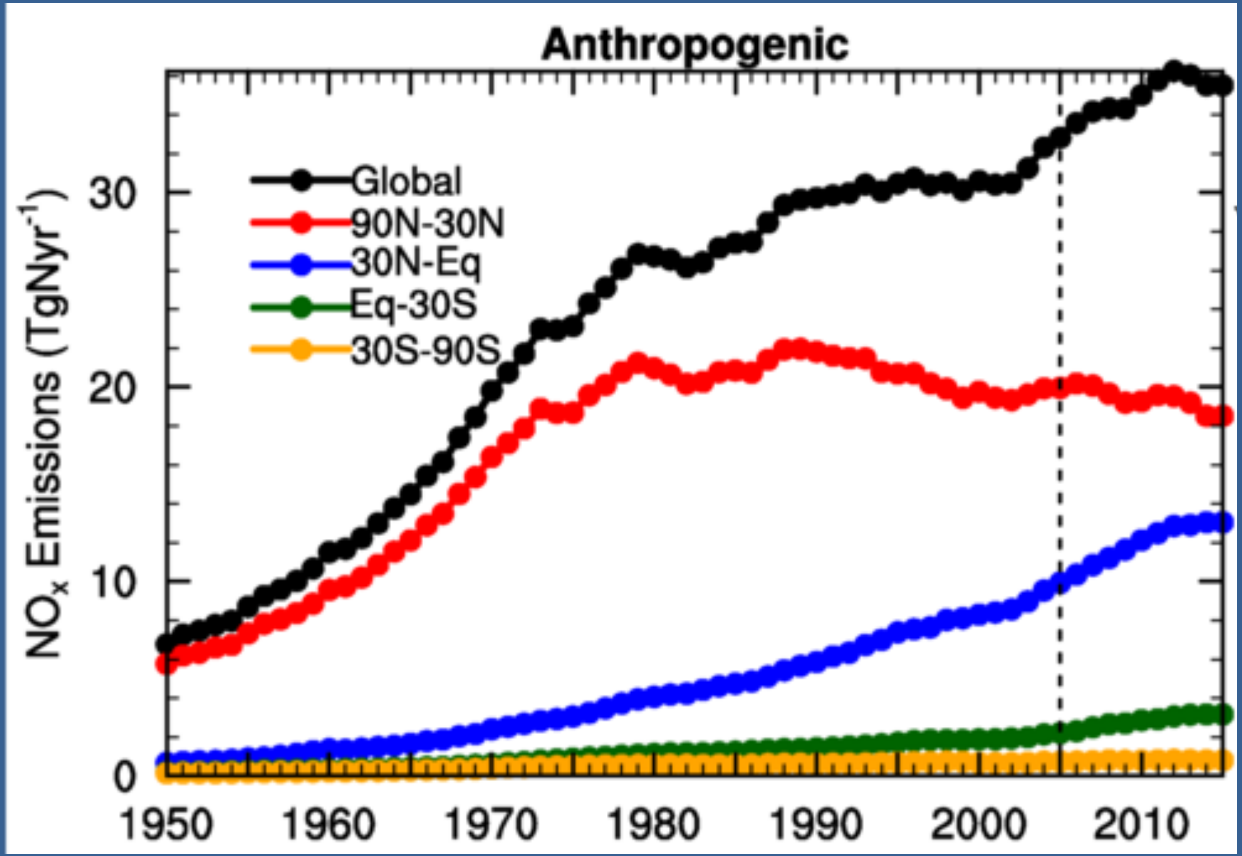

CMIP-6 global NOx emissions have levelled off since 2010

Methane has increased globally by 5% since 2005

Decreases in northern mid-latitudes

Increases in the tropics

Figure produced by NOAA ESRL Global Monitoring Division

Figure produced by Vaishali Naik, NOAA GFDL

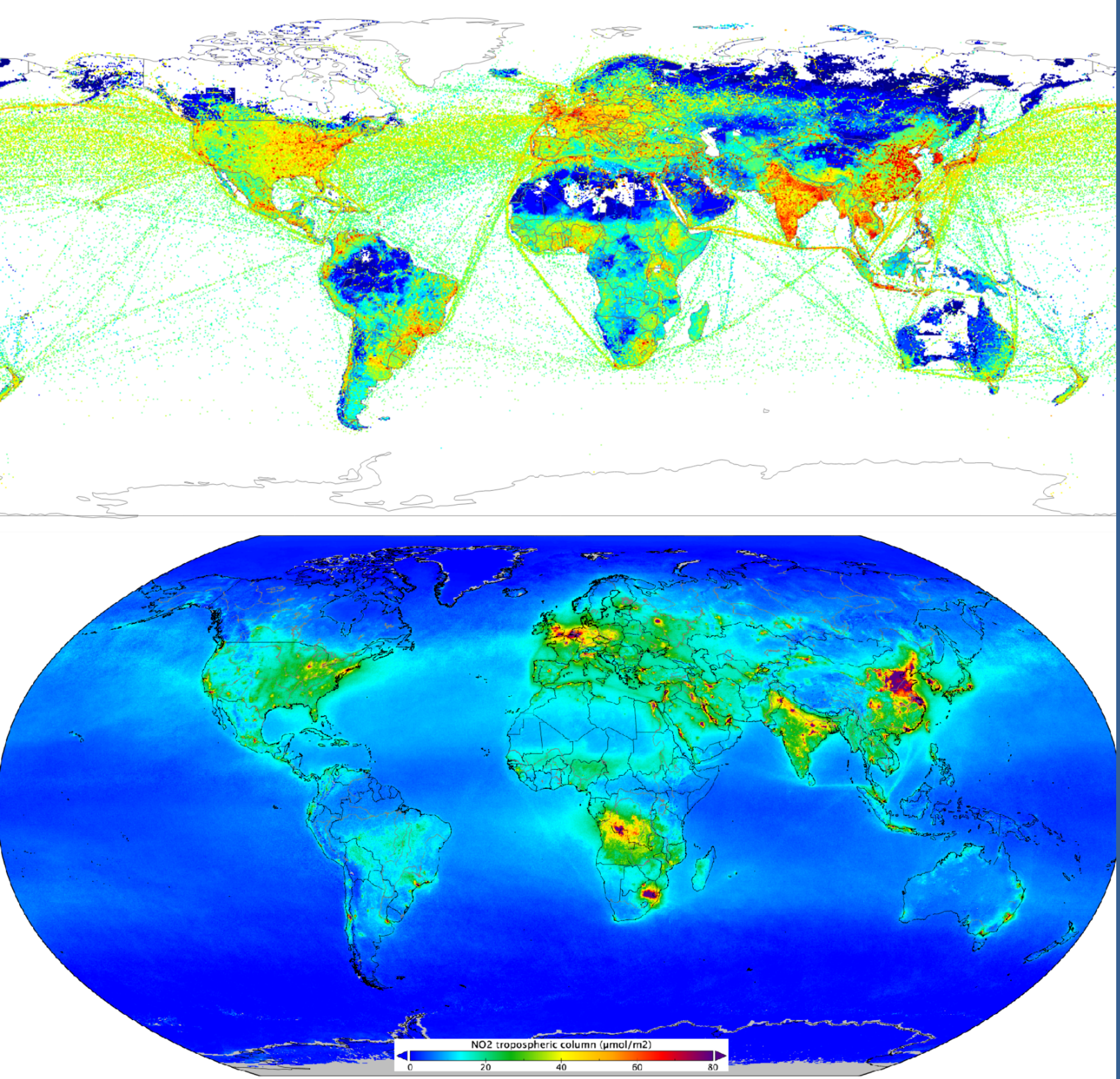

Comparison of CAMS estimates of nitrogen oxide emissions for May 2019 (top) with Sentinel-5P satellite observations for April-September 2018 (bottom). Both datasets highlight the same emission hotspots, as well as clearly showing popular shipping routes. (Copyright Sentinel-5P image: contains modified Copernicus data (2019), processed by KNMI.)(Credit CAMS image: Copernicus Atmosphere Monitoring Service, ECMWF.)

https://atmosphere.copernicus.eu/cams-releases-abundance-emissions-information

2015-2016 minus 2005-2006, for months: 5, 6, 7, 8, 9

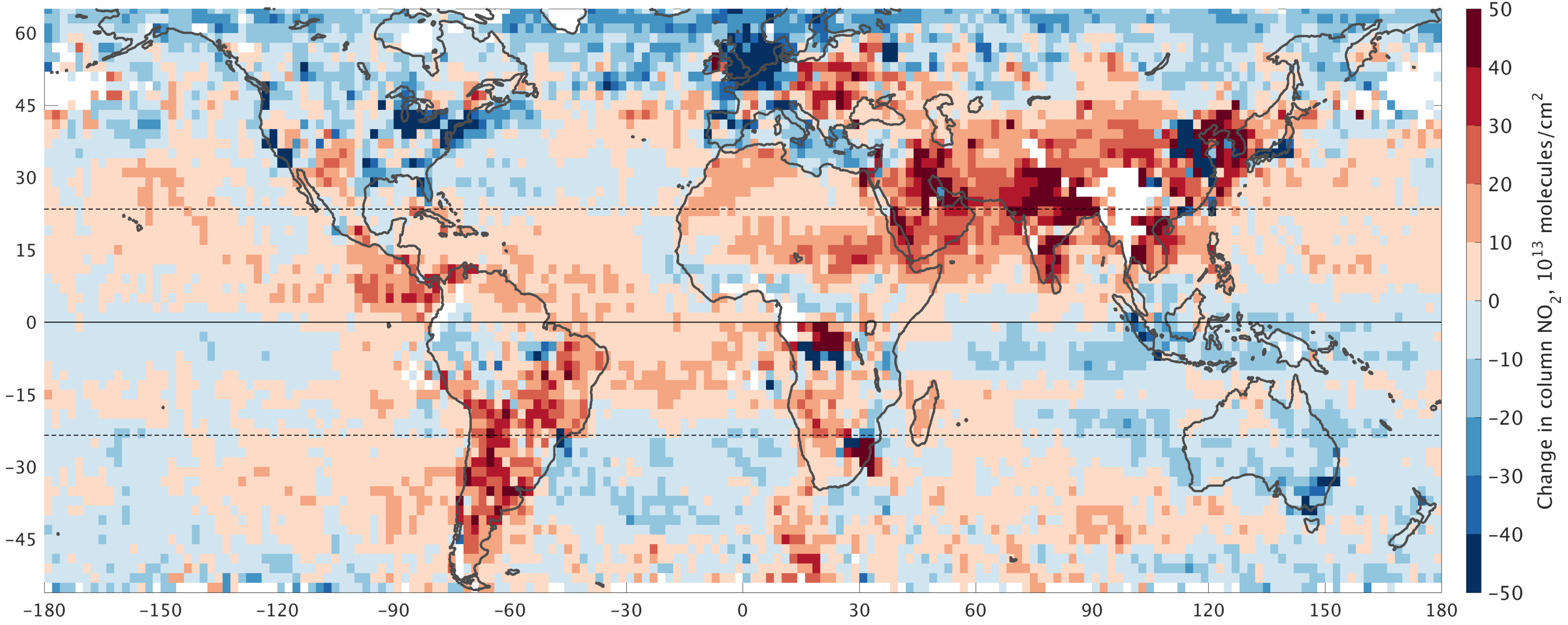

Decadal change of OMI tropospheric column NO_2

Data reprocessed by Folkert Boersma, KNMI to remove the "row anomaly" rows from the entire data set.

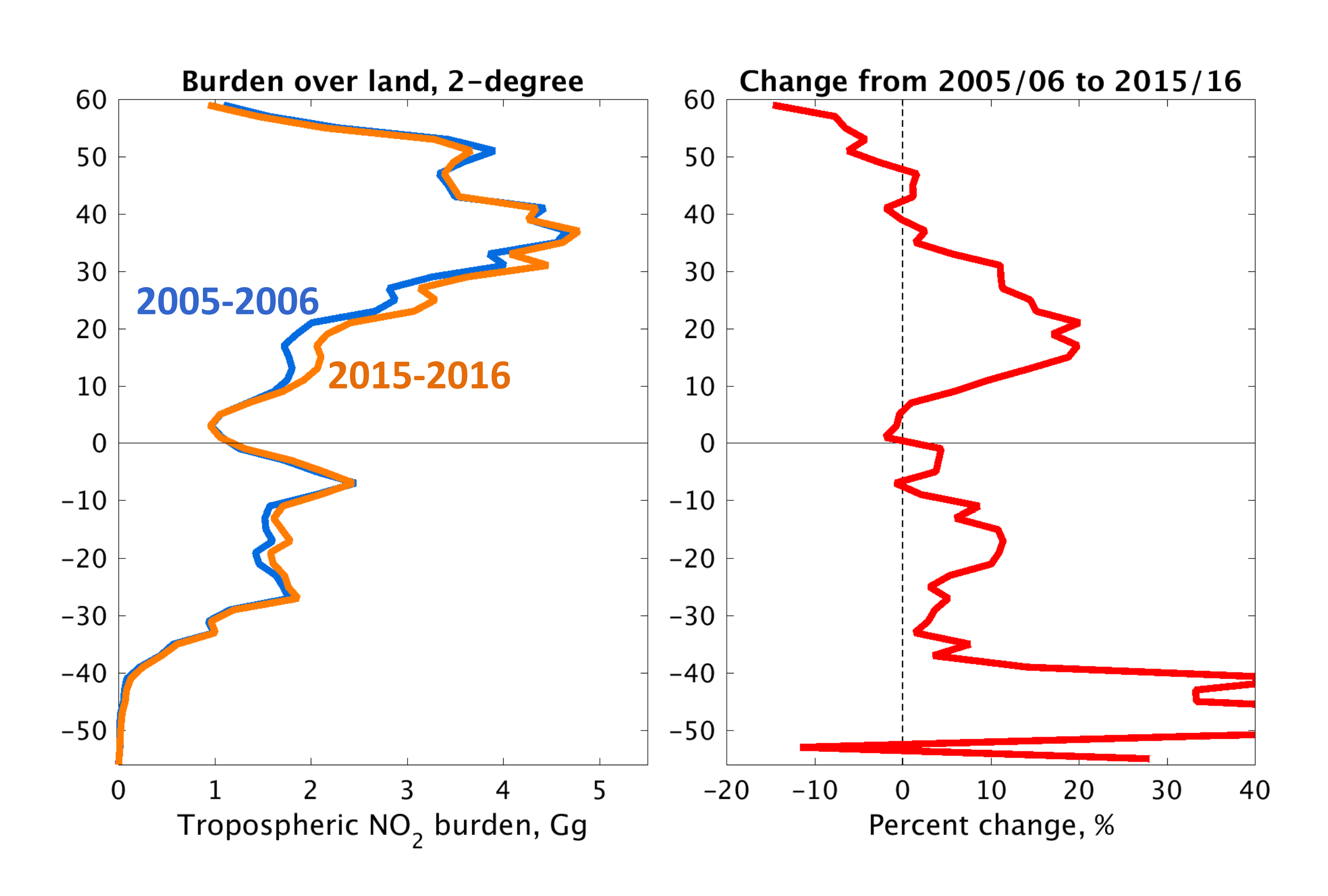

Decadal change of OMI tropospheric column NO_2

Data reprocessed by Folkert Boersma, KNMI to remove the “row anomaly” rows from the entire data set.

nature geoscience
LETTERS
PUBLISHED ONLINE: 7 NOVEMBER 2016 | DOI: 10.1038/NGEO2827

Tropospheric ozone change from 1980 to 2010 dominated by equatorward redistribution of emissions

Yuqiang Zhang[1†], Owen R. Cooper[2,3], Audrey Gaude
Shin-Ya Ogino[6] and J. Jason West[1*]

The global tropospheric ozone burden increased by 9% from 1980 to 2010.

Half of the increase was due to the increase of emissions.

The other half was caused by the equatorward shift of emissions.

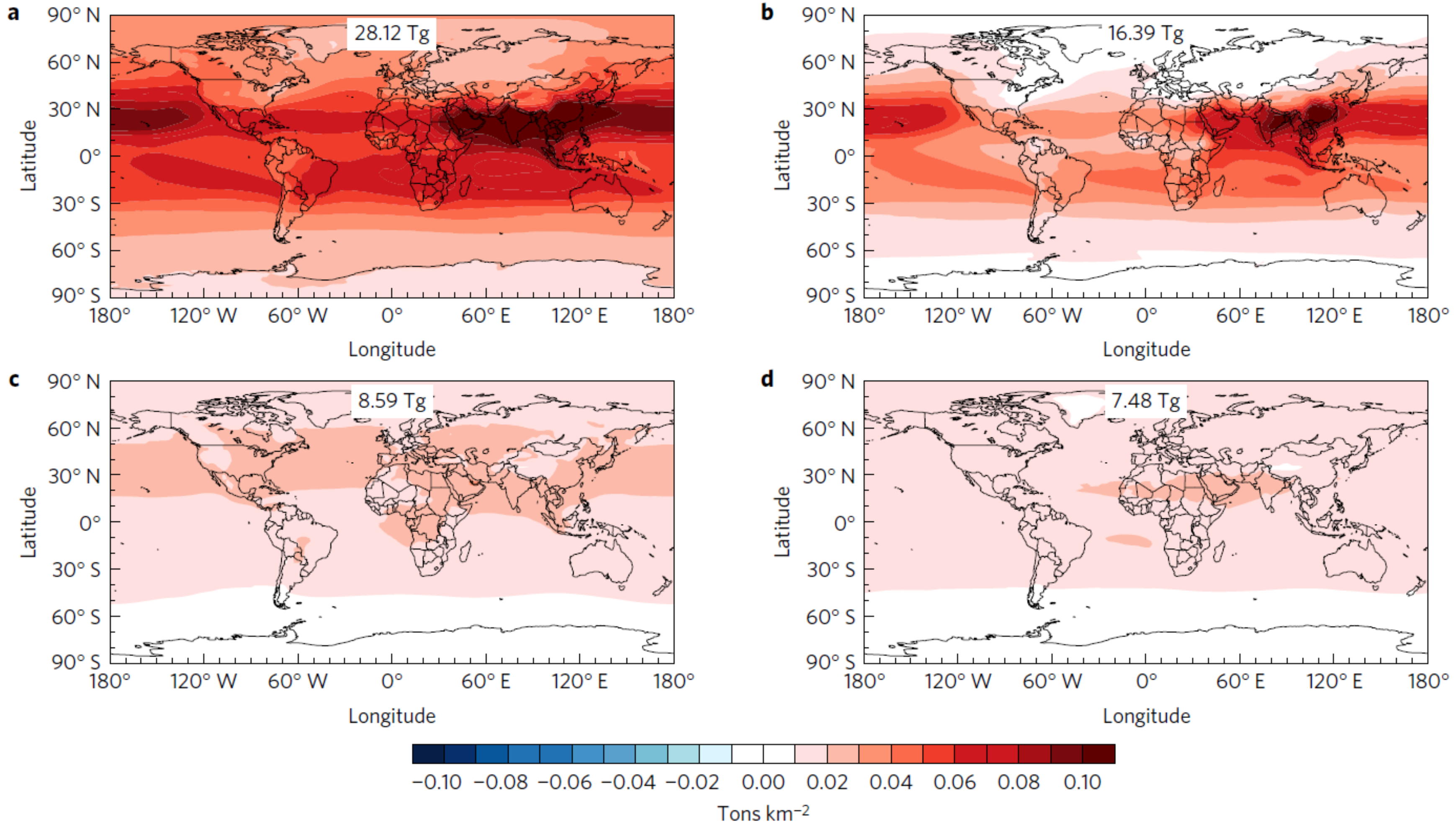

Figure 2 | Spatial distributions for ΔB_{O_3} (tons km^{-2}) from 1980 to 2010. a, Total changes from 1980 to 2010. **b–d**, Influences of changes in the global emissions spatial distribution (**b**), the global emissions magnitude (**c**), and global CH_4 mixing ratio (**d**).

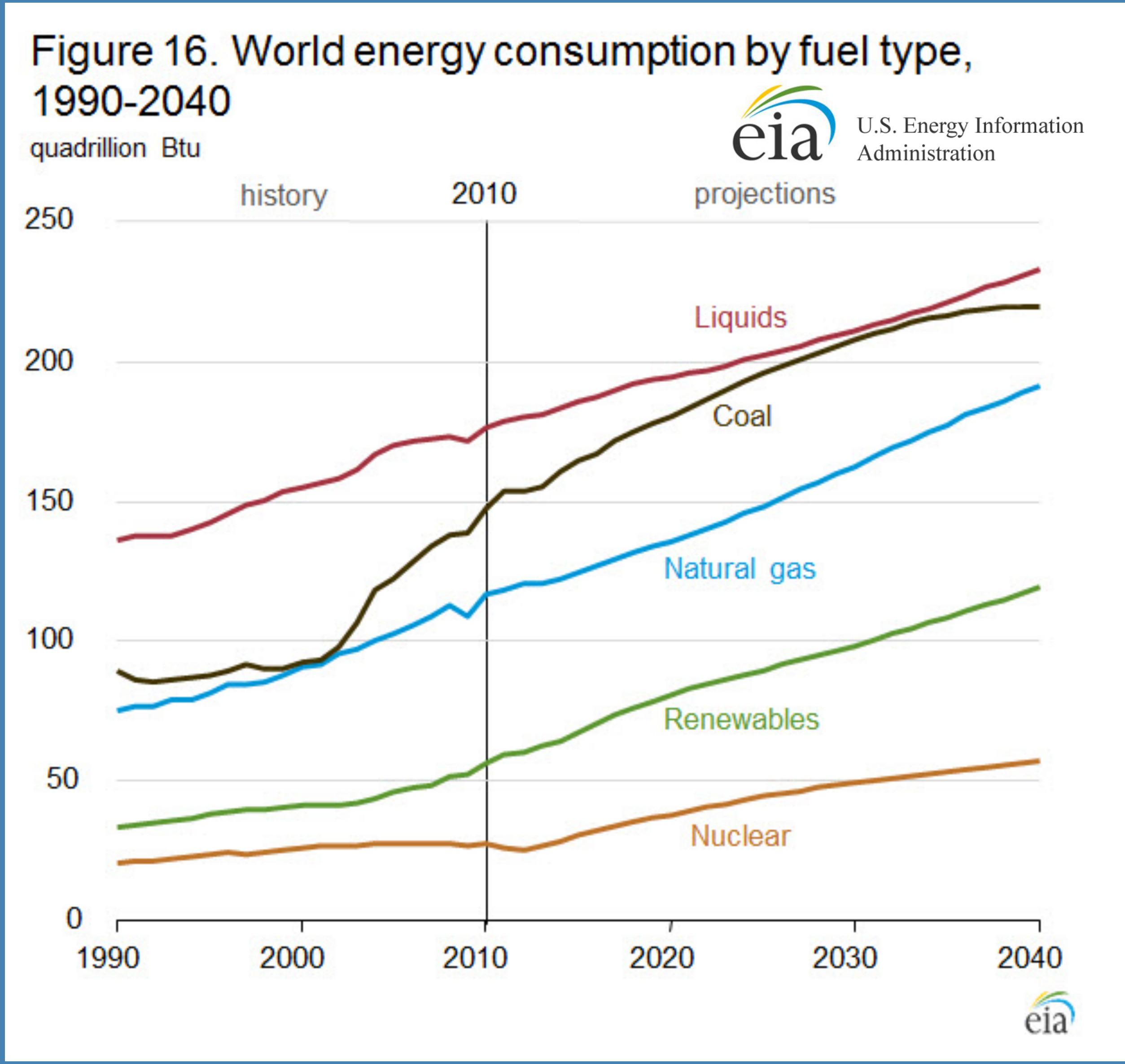

U.S. Energy Information Administration, International Energy Outlook 2013, www.eia.gov/ieo

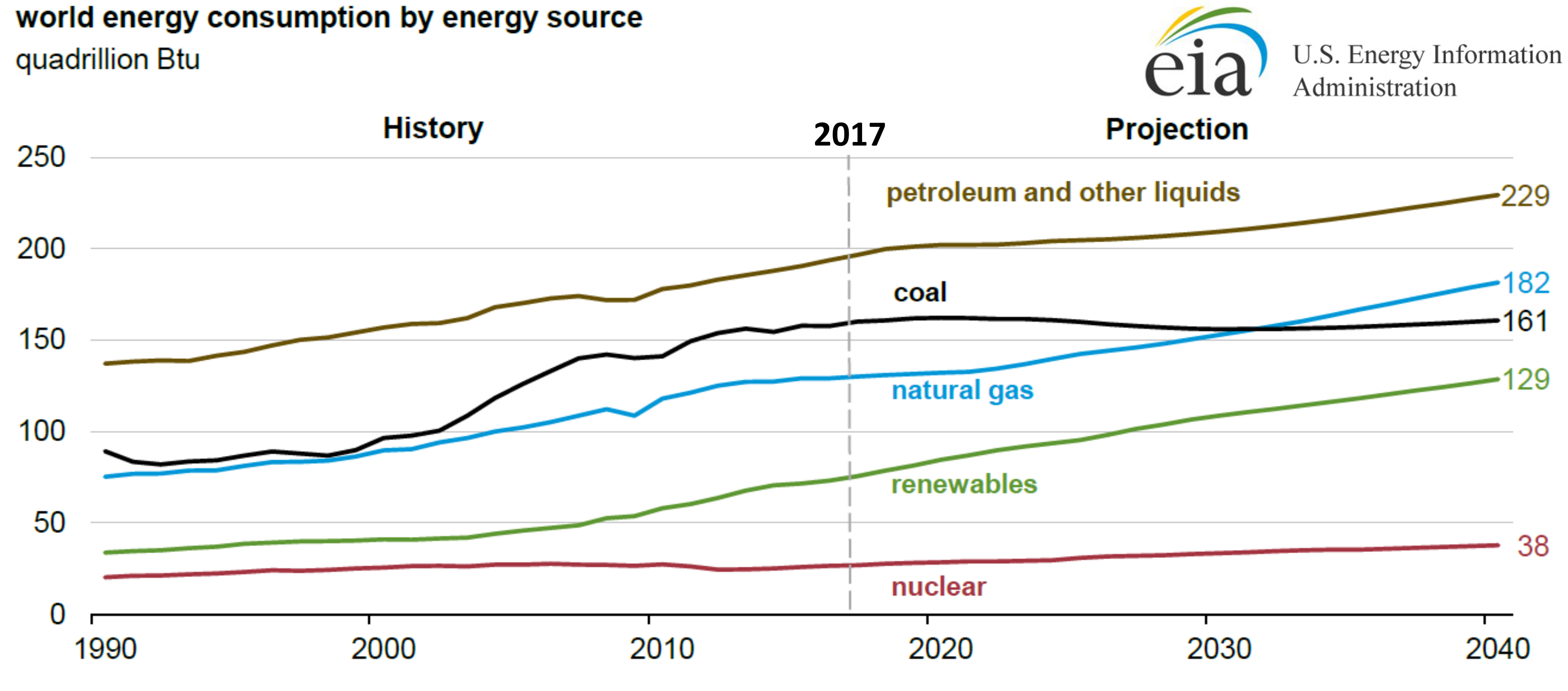

U.S. Energy Information Administration, International Energy Outlook 2018, www.eia.gov/ieo

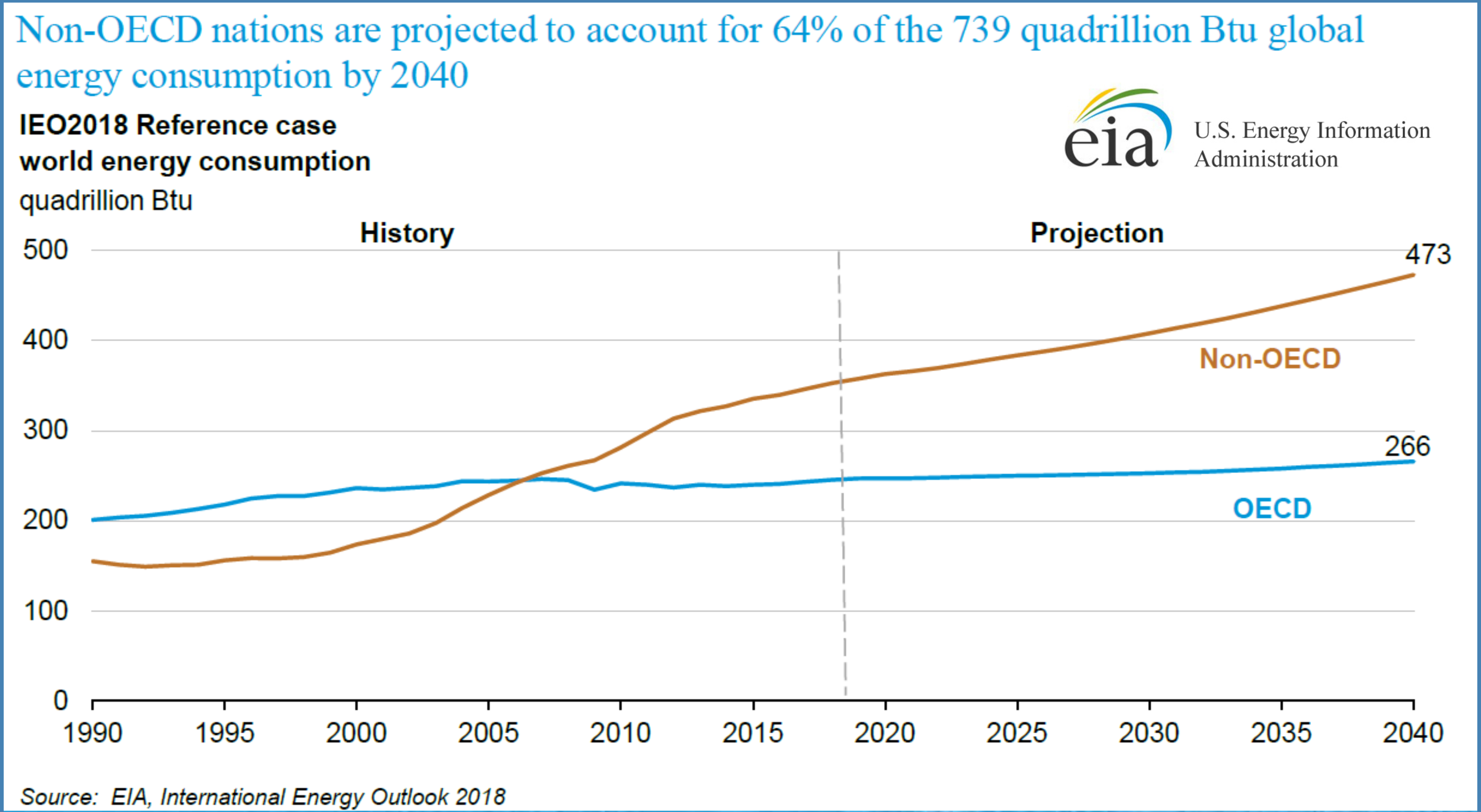

U.S. Energy Information Administration, International Energy Outlook 2018, www.eia.gov/ieo

Asia is projected to have the largest increase in energy use of non-OECD regions

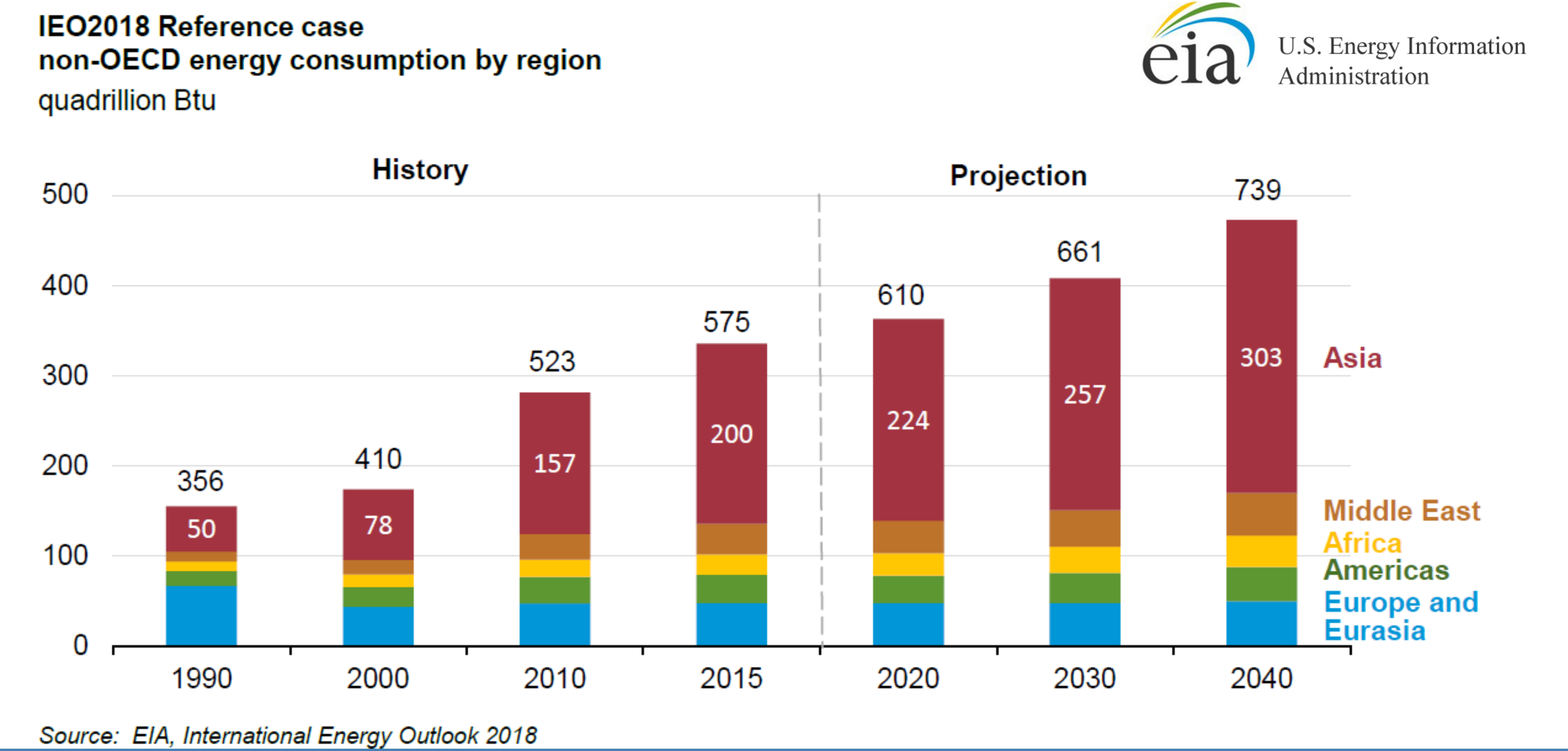

U.S. Energy Information Administration, International Energy Outlook 2018, www.eia.gov/ieo

Tropospheric column ozone for each season as detected by the OMI/MLS product.

Data provided by J. Ziemke, NASA Goddard

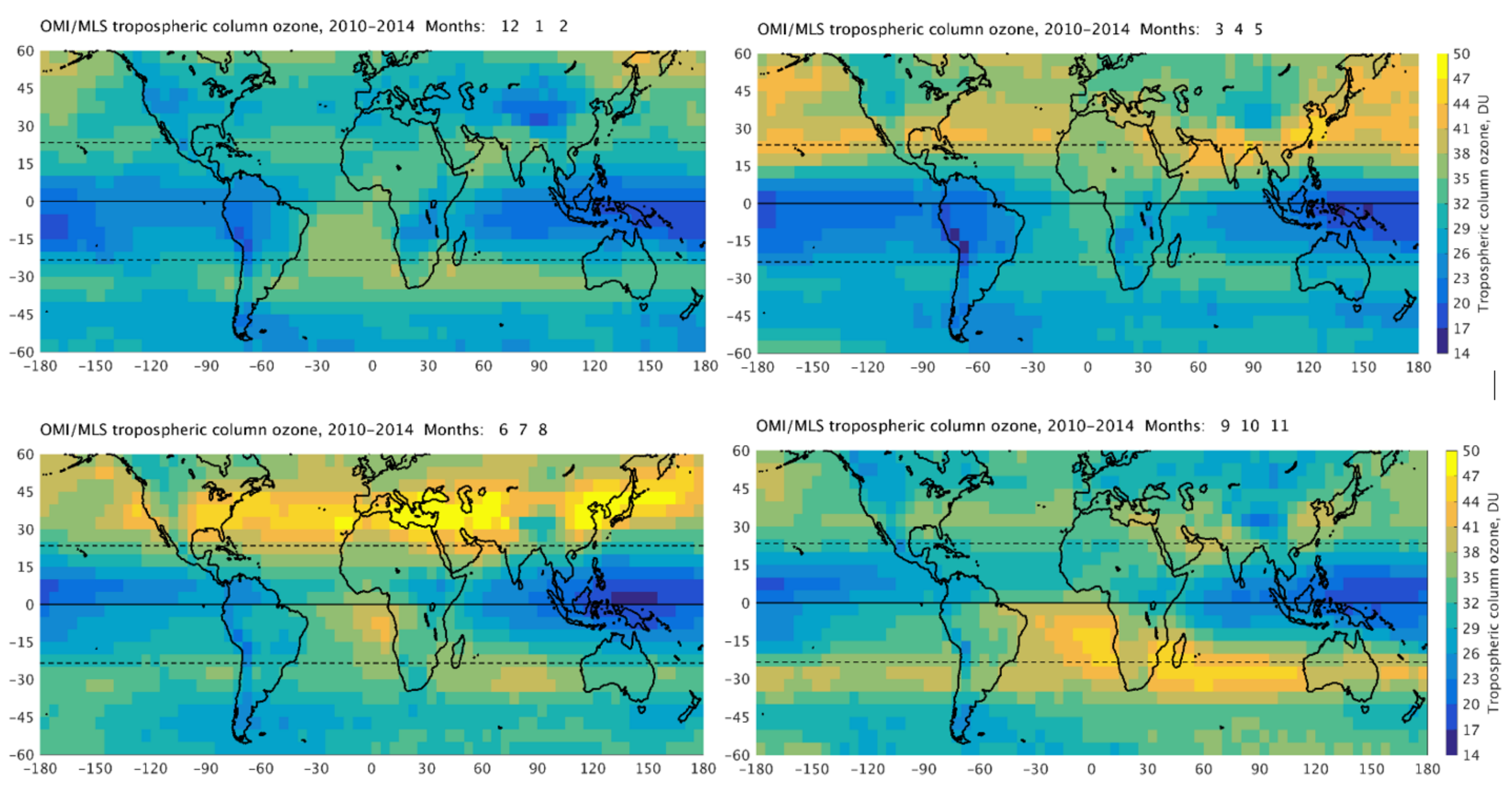

Figure from:

Gaudel et al. (2018), TOAR: Present-day distribution and trends of tropospheric ozone relevant to climate and global atmospheric chemistry model evaluation, Elementa.

First intercomparison of satellite-detected tropospheric column ozone

All annual products show similar features, but with varying intensity.

From:

Gaudel et al. (2018), TOAR: Present-day distribution and trends of tropospheric ozone relevant to climate and global atmospheric chemistry model evaluation, Elementa, 6:39. DOI: https://doi.org/10.1525/elementa.291

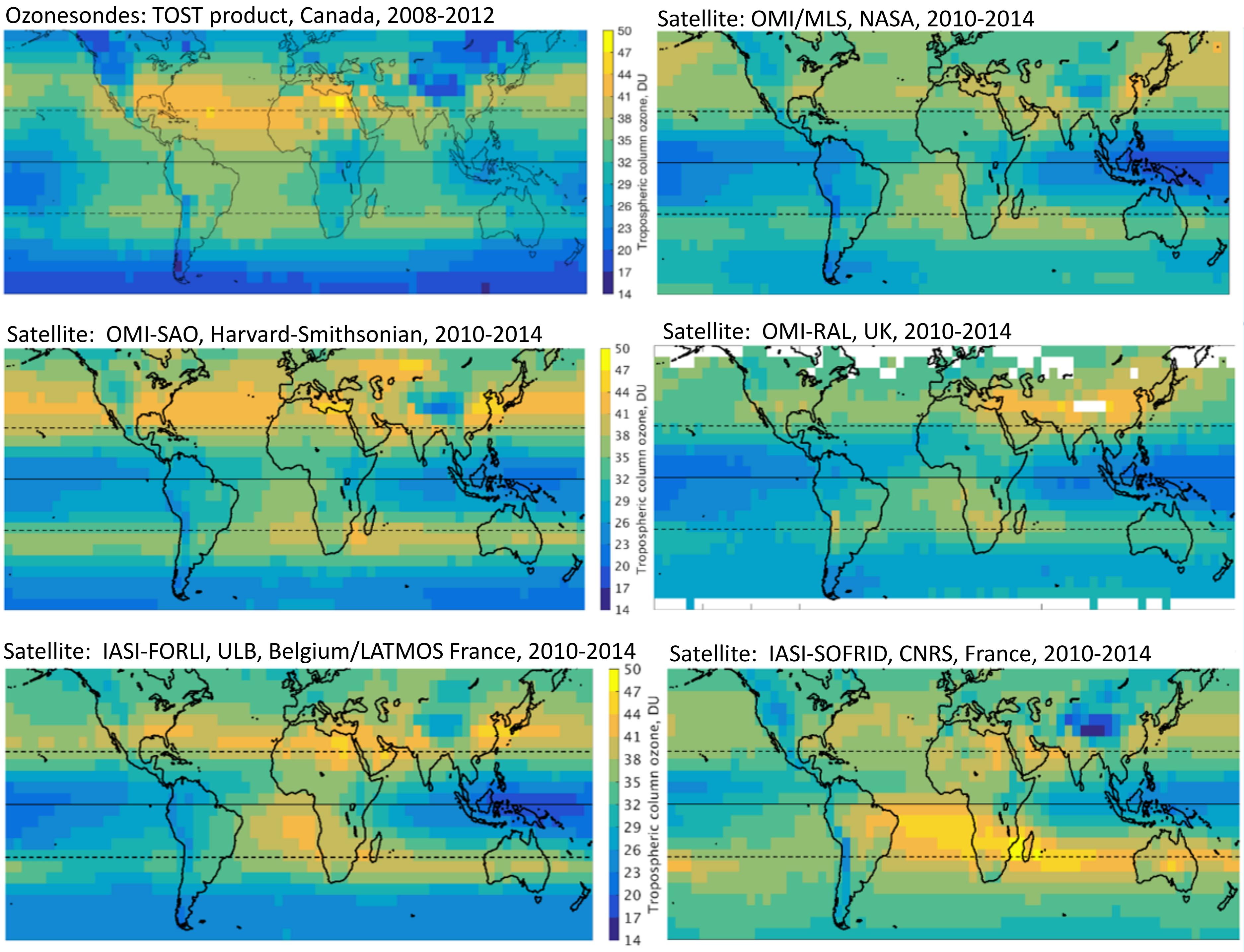

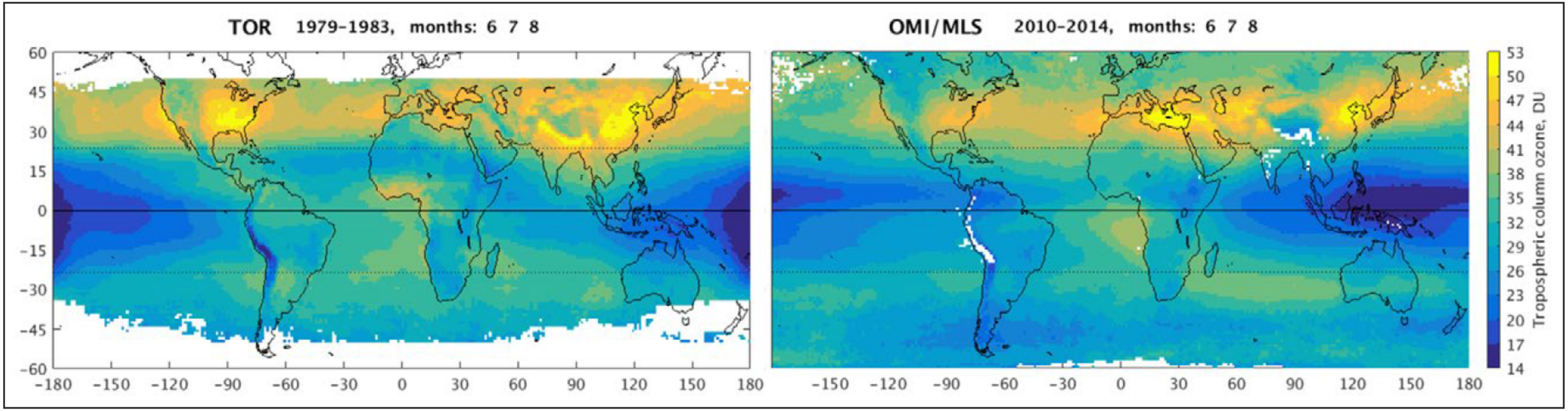

Tropospheric column ozone in 1979-1983 as detected by the TOR satellite product vs. ozone from the OMI/MLS product in 2010-2014.

Data provided by: J. Fishman, *St Louis University/NASA (retired) and J. Ziemke, NASA Goddard*

Figure from: *Gaudel et al. (2018), TOAR: Present-day distribution and trends of tropospheric ozone relevant to climate and global atmospheric chemistry model evaluation, Elementa.*

Atmos. Chem. Phys., 19, 3257–3269, 2019
https://doi.org/10.5194/acp-19-3257-2019

Atmospheric Chemistry and Physics
Open Access

Trends in global tropospheric ozone inferred from a composite record of TOMS/OMI/MLS/OMPS satellite measurements and the MERRA-2 GMI simulation

Jerry R. Ziemke[1,2], Luke D. Oman[1], Sarah A. Strode[1,4], Anne R. Douglass[1], Mark A. Olsen[1,2], Richard D. McPeters[1], Pawan K. Bhartia[1], Lucien Froidevaux[3], Gordon J. Labow[5], Jacquie C. Witte[5], Anne M. Thompson[1], David P. Haffner[5], Natalya A. Kramarova[1], Stacey M. Frith[5], Liang-Kang Huang[5], Glen R. Jaross[1], Colin J. Seftor[5], Mathew T. Deland[5], and Steven L. Taylor[5]

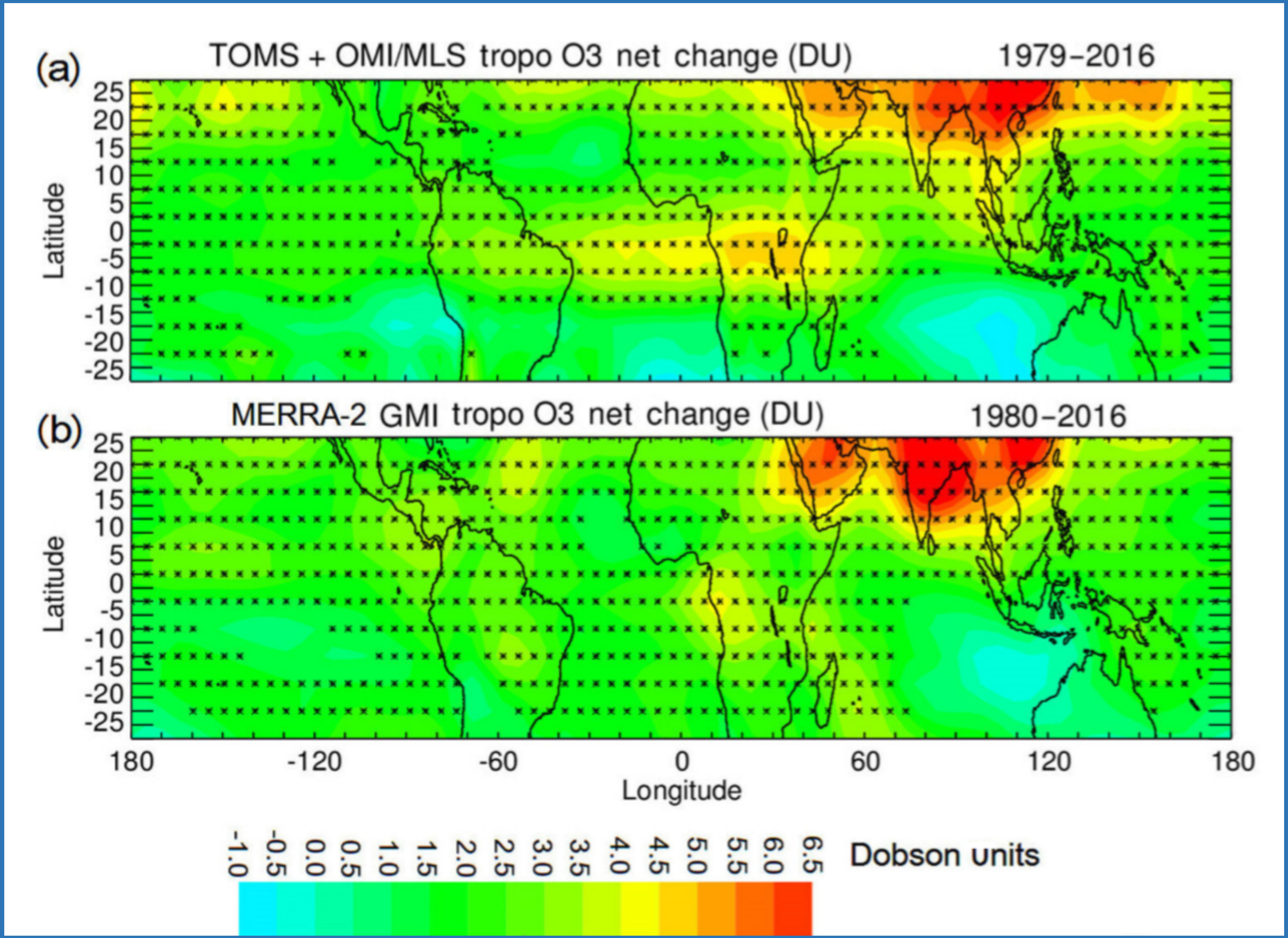

(a)
TOMS + OMI/MLS tropo O3 net change (DU)
1979-2016
(b)
MERRA-2 GMI tropo O3 net change (DU)
1980-2016
Latitude
Longitude
180
-120
-60
0
60
120
180
25
20
15
10
5
0
-5
-10
-15
-20
-25
-1.0
-0.5
0.0
0.5
1.0
1.5
2.0
2.5
3.0
3.5
4.0
4.5
5.0
5.5
6.0
6.5
Dobson units

Severe surface ozone pollution in China: a global perspective

Xiao Lu, Jiayun Hong, Lin Zhang, Owen R. Cooper, Martin G. Schultz, Xiaobin Xu, Tao Wang, Meng Gao, Yuanhong Zhao, Yuanhang Zhang

Published in ES&T Letters, 2018

Figure 2. Comparison of April-September ozone metrics (4MDA8, NDGT70, AVGMDA8, AOT40) between China and the industrialized regions of Japan and Korea, Europe, and the US.

Only sites with at least 3-years of measurements are included.

Values inset are regional mean and standard deviation averaged over the N sites.

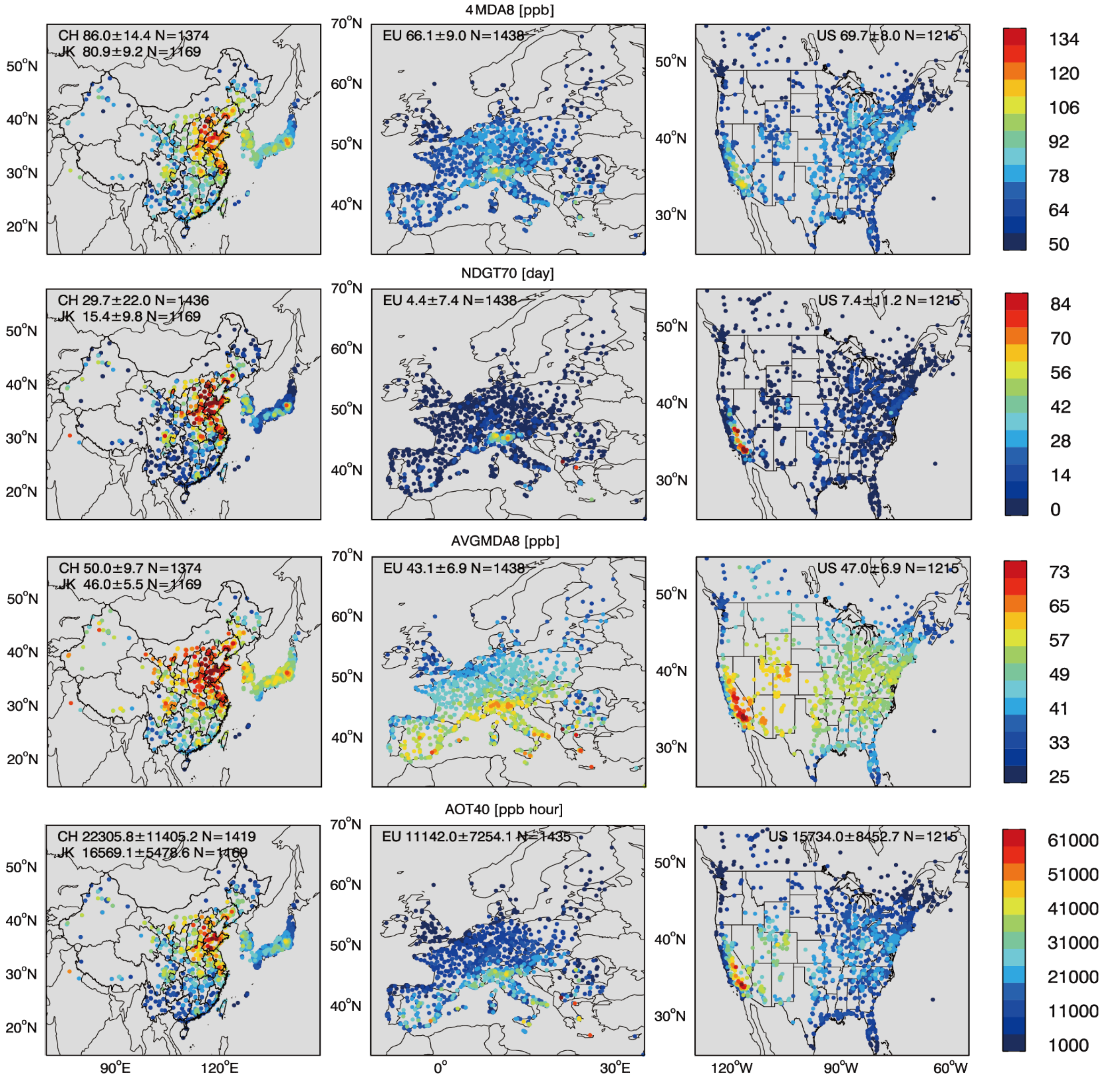

Figure 3 from *Lu et al., 2018*

Evolution of urban surface ozone pollution in China (red), Japan (purple), Europe (orange), and US (blue) from 1980 to 2017.

Also shown are the ozone time series in Beijing (red) and Los Angeles (blue).

Number of available sites is shown in the parentheses.